

Review

# A Perspective of the Design and Development of Metallic Ultra-High Temperature Materials: Refractory Metal Intermetallic Composites, Refractory Complex Concentrated Alloys and Refractory High Entropy Alloys

Panos Tsakiroopoulos 

Department of Materials Science and Engineering, Sir Robert Hadfield Building, The University of Sheffield, Mappin Street, Sheffield S1 3JD, UK; p.tsakiroopoulos@sheffield.ac.uk

**Abstract:** The paper is a personal perspective on the design of metallic ultra-high temperature materials (UHTMs). Specifically, the alloy design “landscape” of metallic UHTMs was considered from the viewpoint of the alloy design methodology NICE. The concepts of synergy, entanglement and self-regulation and their significance for alloy design/development were discussed. The risks, ecological challenges and material-environment interactions associated with the development of metallic UHTMs were highlighted. The “landscape” showed that beneath the complexities of alloy design lies an elegant and powerful unity of specific parameters that link logically and that progress can be made by recognising those interrelationships between parameters that generate interesting, diverse, and complex alloys.

**Keywords:** alloy design; refractory metal intermetallic composites; complex concentrated alloys; high entropy alloys; Nb-silicide-based alloys



**Citation:** Tsakiroopoulos, P. A Perspective of the Design and Development of Metallic Ultra-High Temperature Materials: Refractory Metal Intermetallic Composites, Refractory Complex Concentrated Alloys and Refractory High Entropy Alloys. *Alloys* **2023**, *2*, 184–212. <https://doi.org/10.3390/alloys2030014>

Academic Editor: Yong Zhang

Received: 27 July 2023

Revised: 19 August 2023

Accepted: 25 August 2023

Published: 30 August 2023



**Copyright:** © 2023 by the author. Licensee MDPI, Basel, Switzerland. This article is an open access article distributed under the terms and conditions of the Creative Commons Attribution (CC BY) license (<https://creativecommons.org/licenses/by/4.0/>).

## 1. Introduction

Some time ago, “vision” in alloy design and development was a matter of looking ahead, extrapolating from the present. This is still the case for some material types. Then, the “vision” for the future became blurry because the future would be so unlike the past. Which materials should take us “beyond the nickel-based superalloys”? Should the future be merely the future of the past, based on ideas that dominated metallurgy for many decades? Should the new ultra-high temperature materials (UHTMs) be ceramic and/or metallic? (See Abbreviations).

Risk has a role to play in modern consciousness. Knowledge about risks is dynamic, changing in time and space, and often is the product of the pre-established beliefs and assumptions that individuals bring with them in making their judgements on risk. In engineering communities, risks are linked with certain kinds of value judgements and decision-making. Ideas about risks are shared within a community. Risk ideas often function to protect boundaries, and risk practices can become ways of dealing with unconventionality (nonconformity).

What risks would accompany the new UHTMs? For some, risk was the statistical expectation value of an unwanted event that may or may not happen. Others talked about decisions made under risk, meaning decisions made under known probabilities. Still, others talked about “produced” risks, meaning risks created as the development of materials moved to a more advanced state, i.e., there was a concern for the emergence of new “risk environments” for which we have very little previous experience, do not know what all the risks are and how to calculate them thinking probabilistically.

Alloy design had to “polish” its capabilities for envisaging (and dealing with) different futures so that industry and metallurgical and materials engineering communities had

some idea of what was at stake when the choices the future presented were actually upon us. There was talk about and confusion with strategic planning and scenario planning. Both were influenced by *fomo* (fear of missing out) concerns, by the typical norms, values, and beliefs of different cultures, each with its cultural inheritance, which could change in response to interaction with neighbouring cultures or because of their internal dynamics. Geographical, geological/mining, energy and economic issues, environmental concerns, materials processing, and manufacturing capabilities presented constraints. Scenario planning exploited uncertainties, allowing the creation of “alternative futures”. Strategic planning attempted to minimise uncertainty. Intermetallics, composites and structural ceramics were considered, and later on, refractory metal (RM) alloys were “re-visited” and materials using RMs, namely RM intermetallic composites (RMICs), RM complex concentrated alloys (RCCAs) and RM high entropy alloys (RHEAs), gained popularity, e.g., [1–10]. The toughness property target for new materials with capabilities beyond Ni-based superalloys gave metallic UHTMs the advantage [3,4,7–9].

Alternative scenarios help policymakers think about the future. The consideration of “alternative futures” helped the industry see that the future is shaped not only by the past but by what we think is possible and by our choices. Strategic planning is popular because it is a recognised *modus operandi* that aims to produce assimilated decisions based on predetermined (pre-agreed, pre-established) goals. Scenario planning exploited (made use of) uncertainties, allowing the creation (founding) of “alternative futures”. Strategic planning attempted (endeavoured) to minimise uncertainty. Inputs to scenario planning were more qualitative, and inputs to strategic planning tended to be more quantitative. Scenario planning stimulated (motivated) institutional (methodical) learning. The results of scenario planning were multiple alternative outcomes compared with the quantified single outcome based on the likeliest (credible) scenario, which is the setting for strategic planning. Strategic planning assumed an answer to the question that scenario planning posed. Talk about material/alloy design “landscapes” became widespread. The concept of high entropy alloys (HEAs) was introduced [11,12]. RMICs, RCCAs and RHEAs suggested that the future might not be very much like the past.

### *Alloy Design*

In metallic alloys, there is a strong interdependence of processing, microstructure, and properties across different length scales, linking the atomic with the nano, micro and macro scale, e.g., [13,14]. Such linkages can be established via experiments and characterisation, models, theory, and careful data analysis. Various tools and competencies to design and select new alloys, develop, and improve alloy processing and predict alloy properties are essential for alloy developers, e.g., [3]. An accurate description of thermodynamic properties and alloy systems also is essential, e.g., [13–16].

If all the required linkages, descriptions, models, theories and tools were to be available for alloy design, then (in my opinion) the talk would be about “alloy design topography”. For reasons that will be discussed below, this is currently not possible. Thus, the talk is about “alloy design landscape(s)”. Topography (see Appendix A) is a precise description of topos/place/space/region, while landscape (see Appendix A and below) is a portion of land/territory or its representation, which one can see and comprehend. Interdisciplinary thinking is encouraged by the notion of “alloy design topography” and by the view of “alloy design landscape(s)”. In the former case, the topos (e.g., phase, microstructure, property) becomes a systematically open/communicative concept, the fundamental nature of which and how it might be understood may be questioned and how it might be approached within different disciplinary (e.g., metallurgy, chemistry, physics) frameworks is considered. In the latter case, interdisciplinary thinking is encouraged to build missing linkages and to improve existing ones. In both instances, difficulty rests not so much in developing new ideas but in escaping old ones. Unless we understand the paradigm from which we might have to emerge, we may not be able to free ourselves from the habit of thinking in its terms.

A specific alloy of an alloy system with a known chemical composition can be placed in the phase diagram of the alloy system (provided data for the relevant “composition space” and other phase equilibria data for the alloy system is available, and the phase diagram also is available) using the composition of the alloy [17]. The alloy designer can determine the phases in equilibrium, whether the phases are stable or metastable, and the chemical composition and volume fractions of phases. Alloy designers might especially look for metastable phases. Reliable thermodynamic data is the *sine qua non* of alloy design and development.

The CALPHAD method, first-principles and statistical mechanics calculations can provide a framework to compute thermodynamic properties and phase diagrams and develop thermodynamic descriptions in new “composition spaces”, e.g., [3,13–16,18], but often are inadequate (unsatisfactory, insufficient) to guide alloy developers to design alloys for ultra-high temperature applications. For example, a challenge is presented by high-temperature phases that become unstable at low temperatures (i.e., the thermodynamic stability of high-temperature phases). Another challenge is the stability of microstructures that are contaminated by interstitials. Another challenge is describing the alloy in use/in service and how it interacts with the environment in processing and service, including contamination with interstitials. Irreversible thermodynamics, phase field models and phenomenological approaches can provide some answers and connections. Phenomena at different length scales are key for mechanical properties, as is the effect of interstitial contamination on the mechanical properties of alloys and constituent phases. It is not straightforward to model mechanical properties in a multiscale framework. Calculation/prediction of environmental properties is another serious challenge, as is the inadequate (insufficient, scarce) or non-existent phase equilibria data for RM alloy systems with/without interstitial elements [7,8].

Metallurgists who design new alloys to meet property goals for specific engineering applications face many of the challenges that were outlined above, even for the “well-established” groups of metallic ferrous, superalloy and light metal (Al, Mg, Ti) alloy systems for which there is expertise worldwide and significant volume of data, produced over many decades. On the other hand, the state of affairs is critical regarding metallic UHTMs based on (using) RMs, for example, for metallic UHTMs that could replace Ni-based superalloys in ultra-high temperature applications in a “beyond nickel-based superalloys era”. These metallic UHTMs are RMICs, RHEAs and RCCAs (see Abbreviations). Their microstructures can contain “conventional”, “complex concentrated” or “compositionally complex” (CC), or “high entropy” (HE) phases [9,19,20]. These phases are contaminated with interstitials, some more severely than others, e.g., [19]. These metallic UHTMs must meet specific property goals (targets) regarding toughness, creep and oxidation [4,6,7]. (HEA alloys and HE phases are those alloys and phases where the maximum and minimum concentrations of elements are not above or below, respectively, 35 and 5 at.%, whereas RCCAs alloys and CC phases are those where the maximum and minimum concentrations of elements are above 35% (up to about 40%) and below 5% [8,9,20,21]).

This paper shall consider the alloy design “landscape” of metallic UHTMs from the personal perspective of the alloy design methodology NICE, developed in our research group. I shall discuss the concepts of synergy, entanglement, and self-regulation, their significance for alloy design/development, risk issues and ecological challenges associated with metallic UHTMs, and “give some food for thought”. I shall refer to published data whenever it is appropriate to shed light on the alloy design “landscape”.

## 2. Design of Metallic UHTMs

To meet challenges associated with the development of the aforementioned metallic UHTMs and to better understand the interdependence of processing, microstructure and properties, researchers use different approaches to select alloys to study. Our research group developed a new approach to alloy design called NICE (Niobium Intermetallic Composite Elaboration). NICE presents a methodology to design metallic UHTMs. Methodology

(see Appendix A) is a description of the method. The methodology describes a structured procedure for bringing about a certain goal, e.g., to discover new knowledge, to establish correlations between practice and results, to clarify the structure of data and see phenomena in a new light, to use experimental data with the goal of finding relationships that can be used to make predictions or understand studied phenomena. NICE aspires to assist the metallurgist in designing/selecting metallic UHTMs of alloy systems for which (a) there is a small amount of data about their processing and properties and (b) some phase equilibria data is available or is not available, as is most often the case for RM alloy systems with simple metal and metalloid elements additions, for example, the elements Al, B, Ge, Si, Sn. The latter are key alloying elements to get a balance of mechanical properties and oxidation resistance in metallic UHTMs [7,9,21].

Similarly with the design of steels, light metal alloys (Al, Mg, Ti-based) or superalloys, NICE uses the results of first-principles calculations for phase equilibria data and phase diagrams and the results of experimental studies of alloying behaviour of transition metal (TM) and simple metal alloys, e.g., [22–37]. Within the framework of NICE are developed thermodynamic descriptions in new “composition spaces” to guide alloy developers to design alloys for high-temperature applications, e.g., [38–40]. NICE also has a say about the oxidation of these alloys [7,19,41–47], the contamination of their phases with interstitials, in particular oxygen, and how interstitial contamination affects properties, namely hardness, specific yield strength and Young’s modulus, e.g., [8,20]. Furthermore, NICE uses, when applicable, the latest and new knowledge generated by research (see Section 5.2), considers costs, engineering, and ecological issues (see below) and motivates metallurgists to discover new links between processing, microstructure, and properties, and draws attention to matters that theory and modelling must address. The evolution of NICE for metallic UHTMs with Nb and Si additions and its capabilities was discussed in [7,9,20,21,48]. Most important in NICE are synergy, entanglement (see Appendix A and below) and self-regulation (see Section 6). An objective of NICE is not so much to obtain new data about metallic UHTMs as to discover new ways of thinking about them.

### 3. Synergy

A metallic alloy can be described as a material with a single phase or multiphase microstructure that contains defects and can be chemically inhomogeneous (macro and micro-segregation) and which has a particular “architecture” (size, shape and distribution of phase(s), vol.% of phases), owing to its chemical composition and processing history, which give it its mechanical and/or functional and/or environmental properties that might make the alloy useful or not useful for structural or functional application(s), a topic of discussion(s) or not a hot topic among metallurgists and other interested parties.

Quality is the property of something that exists per se, the property that something has with respect to its inherent nature. There is no one way to define quality. It varies according to the interested party (stakeholder) involved. One defines quality based on one’s perspective of it. Quality has come to mean objectively measurable aspects of something, i.e., quality is about measurable stuff, subjective or inter-subjective (see Appendix A) opinions whether something is “fit for use”, i.e., quality is about the usefulness of something, and also is about something splendid, superb, extremely good and outstanding. The whole, whose quality is considered as this, is something beside the parts or is more than the sum of its parts as it “results from” (“arises”) the latter. In other words, quality is allied with the concept of synergy (see Appendix A).

In this paper, we are interested in metallic alloys, i.e., the something in the previous paragraph is a metallic alloy. For example, its measurable aspects (features, characteristics) could be its mechanical properties. Some might find it useful for (fit for use in) a particular application. For others, it might be an extremely good material. I wish to expand on the idea of the “quality of a metallic UHTM”, in particular, to build on synergy, entanglement, self-regulation and properties in the framework of NICE.

I wish to use an approach employing “human beings reasoning”. The metallic alloy will be described or thought of as having a “human form” or “human attributes”. This approach is, in my opinion, very useful when confronting sustainability, recyclability and “circular economy”, e.g., [49], challenges, and the risks associated with the development of metallic-UHTMs (see Sections 1 and 5–7). In the remainder of this and the next sections, the “equivalent words/phrases in the world of human beings” will be given in parenthesis and/or in italics. For some of these words, I shall also give the Greek equivalent, and for two of the words, I shall give their etymology because, in my opinion, it helps to understand the interconnections that I wish to show. Words that are relevant to this approach are indicated with an asterisk in Appendix A.

An alloy (polis/city, see Appendix A) is an assembly/collection (ecclesia, community, see Appendix A) of elements (persons/πρόσωπα/citizens, see Appendix A) and phases (associations, friendships, families) that coexist in the specific material (the specific locality/area). The alloy (polis/city) is structured *in such a way that it can serve the collective life, enabling its elements (persons/πρόσωπα/citizens) and phases (associations, friendships, families) to share or have certain perspectives in common*, for example, be in stable or metastable equilibrium. The alloy (polis/city) acquires its basic attributes/characteristics from the way its alloying elements (persons/πρόσωπα/citizens) and phases (associations, friendships, families) work together (cooperate and define their culture (see Appendix A), i.e., their way of living together/their way of life), that is to say, they are in synergy.

What does synergy mean? It means “work together”. Type of bonding transfer of charge that nowadays are studied with first-principles electronic structure methods or experimentally, e.g., [29–37,50–52], are examples of how elements work together, i.e., are in synergy. Superalloys and steels are different groups of alloys (poleis/cities) whose differences (different cultures, see Appendix A) are exposed by their properties (distinguishing characteristics, distinctive attributes) that their elements (persons/πρόσωπα/citizens) and phases (associations, friendships, families) bring about/give rise/produce. (The word person (πρόσωπον, see Appendix A) defines a relationship. Human beings only become complete in association with one another [53]. We call culture the way of life of a particular society (see Appendix A). Culture might oblige persons to realise some possibilities while forbidding others).

For instance, the typical pattern of behaviour (the way of life) of elements (persons) in superalloys compels/constrains them to bring about some possibilities regarding properties while forbidding others, e.g., RMs in Ni-based superalloys have a particular partitioning behaviour between the  $\gamma$  and  $\gamma'$  phases and can improve creep, but their use prohibits the reduction of alloy density and the improvement of their oxidation resistance, making the use of environmental coatings unavoidable/inevitable. Ni-based superalloys are susceptible to contamination with interstitials, particularly oxygen, and to internal oxidation owing to environment-material interactions. Risks accompany the use of superalloys. We can say that risk is inherent in *the culture of these materials* or that risk is inseparably tangled with them (*with their cultural norms and habits*). Learning how the superalloys perform in service (*learning about their way of life, i.e., their culture*) in aero-engines enhances perceptions of risk (*improves understanding of risk in their culture*).

The in-service (*cultural*) perspective accentuates the role played by dynamic (*cultural*) processes in identifying risks. Synergy, entanglement and self-regulation link up with risk. I call this interwoven risk or IRIS. Furthermore, entanglement, synergy, and self-regulation are associated with sustainability and recyclability issues. I call this concerted effort ESSERE (see Appendix A). Also, self-regulation, synergy and entanglement are key to correlative environment-material interactions (CEMI). IRIS, CEMI and ESSERE will be topics of future publications.

#### 4. Synergy and Entanglement: The Case for Metallic UHTMs

Let me take this line of reasoning about synergy a step further. In a metallic UHTM, different phases can co-exist. For example, in an RMIC, a bcc solid solution and tetragonal and/or hexagonal 5-3 silicide ( $M_5Si_3$ , where  $M = TM$ ) can coexist with other bcc solid solutions or other silicides (e.g.,  $M_3Si$ ) or other compounds (e.g., Laves phase(s)) [54]. The same phases can co-exist in other alloys (see below). For example, in the case of RM(Nb)ICs, RM(Nb)IC/RCCAs or RM(Nb)IC/RHEAs (see Abbreviations), bcc solid solution(s) can be “conventional”, CC or HE according to their chemical composition, or “normal”, Ti-rich, Si-free according to solute partitioning (see the Appendix B) [7–9,19–21,55],  $Nb_5Si_3$  silicide(s) can be “conventional”, CC or HE according to their chemical composition, or Ti rich or Ti and Hf rich according to solute partitioning (see the Appendix B) [7,8,21,56], other compounds (e.g., A15 phases [54]) can be “conventional”, CC or HE according to their chemical composition [19] and eutectics that contain bcc solid solution and  $Nb_5Si_3$  [57] can be “conventional”, CC or HE according to their chemical composition [7,19,57], for example see the Figures 1–4 and 6 in [58] and the Figures 1–6 in [20]. Such intricateness (see Appendix A) of phases materialises from the correlations/relationships between elements, phases, alloys and their properties. We shall expand on this intricateness below in Section 5, where the concept of entanglement (see the Appendix A) will be introduced, and the choice of this term will become clear. It suffices to say that entanglement is a distinguishing characteristic of a metallic UHTM and its elements and phases. The quality of an alloy ensues from this entanglement. Entanglement is attributed to synergy. Entanglement enables the study of a material in a multiscale framework. Entanglement and synergy are instrumental in identifying areas where interdisciplinary research could focus.

To build on the linkage between synergy and entanglement, I shall use again the “human beings reasoning” to suggest that in an alloy (polis/city) the elements (citizens/persons/πρόσωπα) and phases (associations, friendships, families) *are facing each other as in a personal relationship, they converse about their atomic size, electronegativity, valence electrons, and their parameters  $\delta$ ,  $\Delta\chi$ , VEC, and their enthalpy and entropy that results from their getting together (mixing), and working together (being in synergy).*

In the literature, how is synergy revealed by the aforementioned properties and parameters? The synergy is demonstrated by

- (a) The relationships/correlations between
  - (i) alloy parameters (e.g., Figure 15b in [19], Figure 16 in [48], Figure 14 in [46], Figure 15a in [44], Figure 15 in [45], Figure 19 in [8], Figure 2 in [21], Figures 3 and 4 in [59]),
  - (ii) phase parameters (e.g., Figures 1–4 and 6b in [58], Figure 10a–c in [20], Figure 3 in [9], Figure 8 in [48], Figure 5a,b in [60]),
  - (iii) alloy parameters and alloy properties (e.g., Figure 13 in [8], Figure 6 in [9]),
  - (iv) phase parameters and phase properties (e.g., Figure 5 in [58], Figure 5 in [9]),
  - (v) alloy and phase parameters (e.g., Figure 17 in [7], Figure 6 in [8], Figure 17a in [21]),
  - (vi) alloy parameters and processing (macrosegregation), e.g., Figure 8 in [46],
- (b) the “co-habitation” in parameter maps
  - (vii) of phases (e.g., Figure 3a in [9], Figure 10 in [21]) and
  - (viii) of alloys (e.g., Figure 5 in [7], Figure 19 in [8], Figure 1 in [9]), and
  - (ix) of “conventional”, CC or HE phases (solid solutions, intermetallics) “living together” in the microstructure (Table 11 in [19], Figures 1, 4 and 5 in [20], Figures 1–4 in [58]), and
- (c) the function/role assumed in a particular situation by each parameter separately and by parameters together to give
  - (x) the properties of phases (e.g., Figure 21d,e in [61]) and
  - (xi) the properties of alloys (e.g., Figure 15 in [19]).

The linkage between entanglement and synergy arises from the (a), (b) and (c) in the previous paragraph. Because each parameter (i.e.,  $\delta$ ,  $\Delta\chi$ , VEC, etc.) is related to more than one alloy property, each parameter and thus each underlying physical property (i.e., atomic size, electronegativity, valence electrons, etc.) *has a say/has the “right” or “power” to influence or make a decision* about properties of the alloy (polis/city). The parameters work together/are in synergy for each property. Their importance lies in their *distinctive character and the situation in which each one finds itself*.

The *characteristics, attributes or traits that make up and reflect* what a phase is in an alloy (polis/city) link it with the other phases. For example, a “conventional” solid solution is linked with a CC solid solution with which it coexists (e.g., see Figure 6b,c in [20]) or a CC solid solution is linked with a CC Nb<sub>5</sub>Si<sub>3</sub> with which it coexists (e.g., see Figure 6c in [58]). Thus, the phases in an alloy are in synergy and intricateness (entangled).

The aforementioned linkage between entanglement and synergy was discovered owing to the capacity of the NICE methodology to gain a new understanding of alloying behaviour and properties in metallic UHTMs (see next section). NICE demonstrates that entanglement is a necessity in a metallic UHTM. Furthermore, unknown (“hidden”) relationships between parameters and between parameters and properties of phases are discovered with NICE. To put this another way, the design of alloys using NICE can be improved with the discovery of unknown (“hidden”) relationships, which is possible with this new methodology for alloy design. In the next seven paragraphs, examples are given for such relationships for bcc solid solution, Nb<sub>5</sub>Si<sub>3</sub> silicide, C14-NbCr<sub>2</sub> Laves phase, A15-Nb<sub>3</sub>X (X = Al, Ge, Si, Sn) compounds, maps of alloys and phases, macrosegregation and maps for bond coat alloys for environmental coatings.

Regarding the bcc solid solution,

- (1) for B free RM(Nb)ICs, RM(Nb)ICs/RCCAs and RM(Nb)ICs/RHEAs, there is a gap in  $\Delta\chi_{ss}$  values, see the Figure 4 in [21], Figure 6 in [7], Figure 6 in [55] and Figure 3a in [20], and
- (2) for B containing RM(Nb)ICs, RM(Nb)ICs/RCCAs and RM(Nb)ICs/RHEAs there is a gap in  $\delta_{ss}$  values, see the Figure 8a in [48]. Furthermore, in RM(Nb)ICs, RM(Nb)ICs/RCCAs and RM(Nb)ICs/RHEAs,
- (3) the parameter  $\delta_{ss}$  can differentiate
  - (i) between Si-free bcc solid solution ( $\delta_{ss} < 5$ ) and Ti-rich bcc solid solution ( $\delta_{ss} > 5$ ), see Figure 3 in [21] and Figure 5 in [55], and
  - (ii) the effect of different solutes in CC/HE and “conventional” solid solutions, see Figure 2c in [20], whereas
- (4) The parameter VEC can differentiate the effect of the concentrations of alloying additions on the type of bcc solid solution (meaning “conventional”, or CC/HE) in alloys, see the Figure 3b in [20]. Additionally, there are relationships between parameters of CC/HE and “conventional” bcc solid solution, see Figure 6b in [20], the parameter  $\delta_{ss}$  depends strongly on the  $B_{ss}$  and  $(Ge+Sn)_{ss}$  contents of the solid solution, see the Figure 7 in [20], and the parameters  $VEC_{ss}$ ,  $\Delta\chi_{ss}$  and  $\delta_{ss}$  increase with the concentration of oxygen in the solid solution, i.e., with interstitial content, see the Figure 11 in [20].

Concerning the Nb<sub>5</sub>Si<sub>3</sub> silicide in RM(Nb)ICs, RM(Nb)ICs/RCCAs and RM(Nb)ICs/RHEAs,

- (a) the parameters  $\Delta\chi_{Nb_5Si_3}$  and  $VEC_{Nb_5Si_3}$  can differentiate the alloying behaviour of Nb<sub>5</sub>(Si,X)<sub>3</sub> where X = B, Ge, Sn, and (Nb,Ti,Y)<sub>5</sub>(Si,Z)<sub>3</sub> where Y = TM, RM and Z = Al, B, Ge, Sn, see the Figures 5–11 in [56], and the Figure 6 in [21],
- (b) There are correlations between the parameters  $\Delta\chi_{Nb_5Si_3}$  and  $VEC_{Nb_5Si_3}$ , see Figure 3b–e in [9] and Figures 12 and 13 in [48],
- (c) the steady state creep rate  $\dot{\epsilon}_{Nb_5Si_3}$  and the shear stiffness  $C_{44}$  is correlated with  $VEC_{Nb_5Si_3}$ , see the Figure 5c in [9], and the Figures 15a and 16a in [57], respectively, and

- (d) parameters of the silicide are linked with parameters of the metallic UHTM, e.g., see Figure 7 in [21] and Figure 6a in [58].

The alloying behaviour of the C14-NbCr<sub>2</sub> Laves phase in RM(Nb)ICs, RM(Nb)ICs/RCCAs and RM(Nb)ICs/RHEAs can be described (i) with parameter maps, see the Figures 2 and 3 in [54] and the Figure 17 in [61], and (ii) with solute maps, see the Figure 21 in [21], the Figures 1–4 in [54] and the Figure 18d in [61].

As regards the A15-Nb<sub>3</sub>X (X = Al, Ge, Si, Sn) compounds in RM(Nb)ICs, RM(Nb)ICs/RCCAs and RM(Nb)ICs/RHEAs,

- (a) Their alloying behaviour can be described
- (i) with solute maps, see the Figure 13 in [19], Figure 16 in [61], Figure 14 in [45] and Figure 11 in [62],
  - (ii) with parameter maps, see the Figure 18c in [61], Figure 3f in [9] and Figure 8 in [21],
- (b) there is a gap in VEC<sub>A15</sub> values, see the Figure 3f in [9], Figure 6 in [54], and Figure 9 in [21],
- (c) their hardness depends on the parameters VEC<sub>A15</sub> and  $\Delta\chi_{A15}$ , see the Figure 21d in [61], and the Figures 7 and 8 in [54], and
- (d) they improve oxidation resistance in synergy with other phases, e.g., see the Figure 12c in [42].

Regarding eutectics with bcc solid solution and Nb<sub>5</sub>Si<sub>3</sub> silicide in RM(Nb)ICs, RM(Nb)ICs/RCCAs and RM(Nb)ICs/RHEAs

- (1) Their alloying behaviour is described
- (i) with parameter maps, see the Figures 1–5 in [57] and the Figure 17c in [21], and
  - (ii) with solute maps, see the Figures 6, 8–10 and 14 in [57],
- (2) There are gaps in the values of the parameters  $(\Delta H_{\text{mix}})_{\text{eutectic}}$  and  $\Delta\chi_{\text{eutectic}}$ , see the Figures 3 and 4, respectively, in [57] and
- (3) Their hardness depends on VEC<sub>eutectic</sub>, see the Figure 12a in [57], and on  $\Delta\chi_{\text{eutectic}}$  and  $\delta_{\text{eutectic}}$ , e.g., see the Figure 15 in [21].

With reference to macrosegregation (MAC) of solutes (X) in RM(Nb)ICs, RM(Nb)ICs/RCCAs and RM(Nb)ICs/RHEAs produced using cold hearth melting and casting, the effect of solute additions on MAC<sub>X</sub> was discussed in [61]. The dependence of MAC<sub>X</sub> on parameters was shown in the Figure 11 in [7], Figures 4–6 in [48], Figure 8 in [46], the Table 7 in [19], Table 6 in [61], Table 8 in [48], Table 5 in [46], Tables 4–6 in [45], Tables 4–6 in [45], Tables 16–18 in [42], the Table 2 in [62] and the Figure 6 in [63].

Regarding the presentation of the alloying behaviour of alloys and their phases in parameters maps,

- (a) alloy maps were shown in the Figure 2 in [21], Figures 1 and 2a,c,d in [9], Figures 1 and 2 in [59] and Figure 19 in [8],
- (b) phase maps were shown in the Figure 16 in [8], Figure 10 in [21], Figure 3a in [9] and Figure 5 in [7] (note that in Figure 5 in [7], the labels for the A15-Nb<sub>3</sub>X and C14-NbCr<sub>2</sub> phases were swapped by mistake),
- (c) maps of alloys and their bcc solid solutions were shown in the Figure 5 in [21], Figures 3–5 in [59], and
- (d) maps for bond coat alloys for environmental coatings were shown in the Figure 13 in [64] and Figure 8 in [9].

Let us return to the coexistence of phases in a specific material. A metallic UHTM (i.e., an RMIC, RCCA or RHEA) can have a bcc solid solution and M<sub>5</sub>Si<sub>3</sub> silicide. Another metallic UHTM with the same solute elements but at different concentrations can also contain bcc solid solution and M<sub>5</sub>Si<sub>3</sub> silicide, not necessarily of the same chemical composition as the first metallic UHTM. There is entanglement in the latter and entanglement in the second metallic UHTM (regardless of where the alloys are/were studied, by whom they are/were



studied or when they are/were studied). The same would be if the second metallic UHTM with the same solute elements and different concentrations consisted of bcc solid solution,  $M_5Si_3$  silicide and another phase, say an A15 compound.

Examples of the outcomes of entanglement in metallic UHTMs with different solutes, which were prepared and studied by different researchers at different locations and at different times, are shown in the Figure 12a in [42], Figures 1 and 14a,c in [43], the Figure 14 in [46], the Figure 15a in [44], in Figure 15a in [46], and in Figure 16 in [21], the Figure 21 in [48], the Figures 11 and 14b,d in [43], and the Figure 12b in [42] as regards isothermal oxidation, respectively at 800 and 1200 °C.

The synergy of solute elements can lead or not lead to meeting a specific property goal. For example, see the Figure 12 in [36] and Figure 7a,b in [7] for the creep of alloyed  $Nb_5Si_3$ , the Figure 15a in [46] for oxidation of alloys, and the Figure 15 in [45] that shows how alloying shifts the alloys in the  $\delta$  versus VEC map in the direction of improved oxidation resistance. Other examples of outcomes of synergy and entanglement on properties of alloys and their phases and vol.% of phases are shown in the Figure 15a–c in [19], in Figures 18 and 21e in [61], the Figures 4, 5a,b and 6 in [9], the Figures 17 and 18 in [48], the Figures 11, 15 and 22 in [21] and the Figure 13c in [55].

In Section 3, I used as an example superalloys and steels as two different groups of alloys (different poleis/cities, see the Appendix A) whose differences (different cultures, see the Appendix A) are exposed by their different properties. Once different types of the said alloys were developed, metallurgists never ceased to change and develop further these alloys (this is history in the “human beings reasoning”). To understand these “cultural changes” and “history”, it is not enough to comprehend the interaction of elements, etc., but it is also necessary to consider the interaction of ideas and theories as well as the “glue” that binds together large numbers of individual researchers and research groups.

What kind of differences (different cultures) would emerge in alloys (poleis/cities), the microstructures of which consist of coexisting “conventional”, CC or HE phases? How would the microstructures (structures) of such alloys (poleis/cities) evolve in service? What would the role of interstitial contamination be in in-service evolution? Would one phase type dominate/be stable? Would it be more important to know the consequences of interstitial contamination, e.g., on phase equilibria and/or properties, than its causes?

## 5. The Alloy Design “landscape” in NICE

With the approach to alloy design instigated with NICE, one can calculate the chemical composition of an alloy to meet “on demand” a specific property goal (target) for metallic materials (in other words, the starting point in alloy design using NICE always is a property goal) [7,9,45–47,64–69], see the Figure 15 in [7] and Figure 1. NICE also calculates

- (a) macrosegregation (MACX) of solute addition(s) X for liquid route processing of the alloy (e.g., for cold hearth melting/casting [70]), and thus can guide to some extent the alloy developer about processing,
- (b) properties of the alloy (hardness, density, specific strength, creep, oxidation),
- (c) the chemical composition of alloy phases,
- (d) the volume fraction of phases and
- (e) mechanical properties of phases, and links
  - (i) the alloy with its phases and vice versa, and
  - (ii) the alloy properties and phase properties.

Experiments can validate or disprove the calculations/predictions (a) to (e).

The linkages (i) and (ii) in the previous paragraph are possible because there are parameters that link alloy, phases and properties. The parameters are based on atomic size ( $r_i$ , parameter  $\delta$ ), electronegativity ( $\chi_i$ , parameter  $\Delta\chi$ ), valence electrons (parameter VEC), enthalpy (parameter  $\Delta H_{\text{mix}}$ ), entropy (parameter  $\Delta S_{\text{mix}}$ ) and  $\Omega (=T_m\Delta S_{\text{mix}}/|\Delta H_{\text{mix}}|)$  [7,54–59], which are the same parameters that are used for the study of HEAs, rapidly solidified alloys, or bulk metallic glasses, e.g., [71], and the ratios sd/sp (concentration of sd over sp electronic

configuration elements) and Nb/(Ti+Hf) [7,47,59,72], which (the ratios) together with the aforementioned parameters are important for properties of RM(Nb)ICs, RM(Nb)IC/RCCAs, RM(Nb)IC/RHEAs [7–10,19–21,47,48,59,73], and their phases [9,21,48,54,56,57,60,61,74]. (For the calculation of the said parameters for alloys and solid solutions, see [55,59], and for the calculation of the parameters  $\Delta\chi$  and VEC of Nb<sub>5</sub>Si<sub>3</sub>, C14-NbCr<sub>2</sub> Laves phase and A15-Nb<sub>3</sub>X (X = Al, Ge, Si, Sn) compounds see [54,56]).

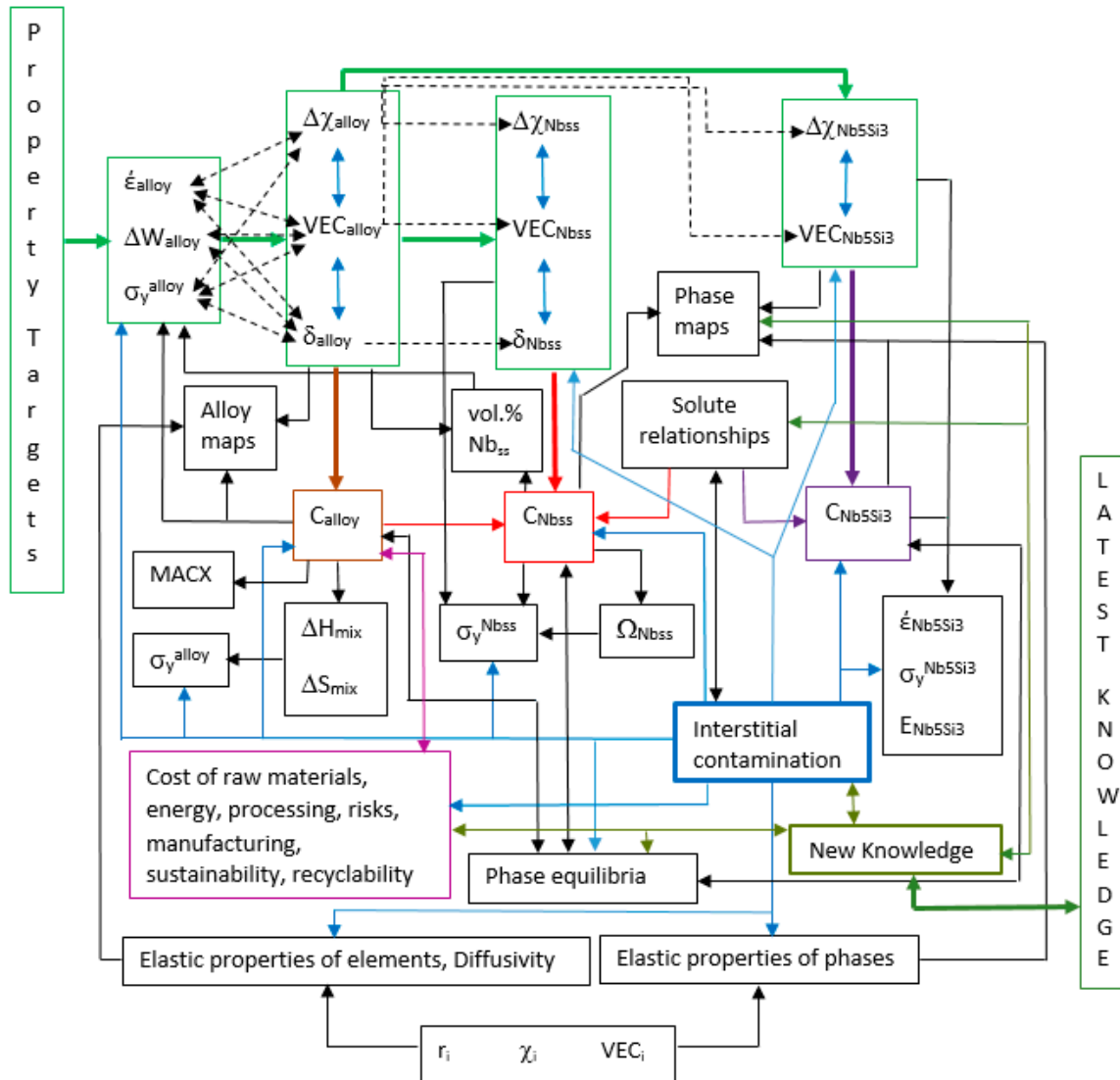


**Figure 1.** Representation of alloy design “landscape” drawn with NICE for a metallic UHTM with bcc solid solution and 5-3 silicide of Nb. VEC is valence electron concentration,  $r$  is atomic size,  $\chi$  is Pauling electronegativity,  $\Delta H_{\text{mix}}$  is enthalpy of mixing,  $\Delta S_{\text{mix}}$  is entropy of mixing,  $\Delta W$  is mass change in oxidation,  $E$  is Young’s modulus,  $\sigma_y$  is yield strength,  $\dot{\epsilon}$  is steady state creep rate,  $\Delta\chi$  parameter based on  $\chi$ ,  $\delta$  parameter based on  $r$ ,  $\Omega$  is parameter based on melting temperature,  $\Delta S_{\text{mix}}$  and  $\Delta H_{\text{mix}}$ , MACX is macrosegregation of element X, and  $C$  is chemical composition.

The term landscape refers to either natural scenery or its representation. Used as representation, a landscape could help one to imagine what an alternative future state of affairs might be like. A landscape can have a dynamic and complex character. It can give information about the relative position of things, define spatial boundaries and delimit particular areas. Also, a landscape can have a “substructure” and a “superstructure”. We orient ourselves in the world by walking around. Things can be seen from different points of view (perspectives). To get a view (impression) of a particular landscape and a perspective

of the land, we have to take a position in it. We become familiar with it by walking around. We can have a survey perspective and a route perspective of the landscape. It makes a difference if we plan our route on a map or navigate our way following noteworthy landmarks on the ground. Seen from a distance, the same scenery might not make a great impression. A landscape is experienced essentially by our moving through it.

Figure 1 shows an alloy design “landscape” for metallic UHTMs that has been produced (“drawn”) with NICE. It is a developing but not yet fully formed “landscape”, i.e., it is a “landscape” *in statu nascendi* (in a state of being born). Economic, engineering and ecological issues, phase equilibria, properties, knowledge and know-how make up a “substructure” that supports the “superstructure” of alloys, their phases and properties. For reasons of simplicity, the “landscape” shown in Figure 1 is about alloys with microstructures that consist of two phases, namely bcc Nb solid solution ( $\text{Nb}_{\text{ss}}$ ) and 5-3 silicide of Nb ( $\text{Nb}_5\text{Si}_3$ ), i.e., for RM(Nb)IC, RM(Nb)IC/RCCA or RM(Nb)IC/RHEA, and for RCCA or RHEA with Nb and Si additions. It can be expanded to include the said two phases plus other compound(s), for example, Laves phases and/or A15 compounds [54], or to be the “landscape” for a material system for an application at ultra-high temperatures, for example, a substrate alloy with an environmental coating [9]. The “landscape” in Figure 1 has “lines and paths”, “focal points”, and “transitions” shown with lines single or double arrows of different weights and colour.

Let us view together the “landscape” in Figure 1. We start from the “superstructure” of alloys, their phases and properties. First, we shall view it from a survey perspective. The “landscape” includes elements, phases, alloys and properties, parameters of alloys and phases, compositions of alloys and phases and links the aforementioned with single or double arrows of different weights and colours. Second, we shall view the “landscape” from a route perspective. One route perspective is to follow the solid, thick green arrows that link boxes delineated with thin green lines. The first two boxes are earmarked for properties. The following three boxes are set aside for alloys, solid solutions and 5-3 silicides. This route starts from properties and takes us first to alloys, solid solutions, and 5-3 silicides. A second route perspective is to follow the green arrows at each of the latter three boxes, change course and follow the direction of the brown, red or purple solid thick arrows.

Another survey perspective shows that the “landscape” includes properties of elements, maps of alloys and phases, and links between the aforementioned and with boxes noted with the previous survey perspective. A third route perspective continues from the alloy composition delimited by the brown box and takes us to alloy maps, alloy properties and macrosegregation of elements (MACX). A fourth route perspective continues from the solid solution composition demarcated by the red box, taking us to phase maps and solid solution strength. A fifth route perspective continues from the silicide composition delineated by the purple box, taking us to phase maps and silicide properties. A third survey perspective shows that the “landscape” includes interstitial contamination (outlined with a blue box) that links with the alloy and its phases (links displayed with light blue arrows).

Next, we consider the “substructure” that is made up of economic, engineering, and ecological issues, phase equilibria and properties, interstitial contamination and new knowledge and links with the latest “external” knowledge, and which (the “substructure”) supports the “superstructure” of alloys, their phases and properties. A fourth survey perspective shows that there are costs associated with the raw elements used in the alloy, as well as energy, processing, manufacturing, sustainability, recyclability, and risk issues that must be considered (shown with a light purple box). A fifth survey perspective reveals that the phase equilibria link with alloy and its phases and with interstitial contamination, and a sixth survey perspective discloses that the latest knowledge and know-how “feeds in” new knowledge, which in turn links with other parts of the substructure and with the superstructure.

A sixth route perspective starts from the interstitial contamination box, links (i) with phase equilibria that are also linked with the alloy and its phases, (ii) with the elastic

properties of elements and their diffusivities in RMs, and (iii) with the elastic properties of phases, and also links with the chemical composition and properties of alloys, then with the chemical composition, parameters and properties of the solid solution and finally with the chemical composition, parameters and properties of the silicide. In this route, we note (a) that phase equilibria are linked with alloy and phases with double arrows, (b) that interstitial contamination is linked with costs, engineering, ecological, and risk issues and (c) that new knowledge is linked with all parts of the landscape via its links with interstitial contamination, phase equilibria, and costs and engineering, ecological and risk issues.

The views of the “landscape” from survey and route perspectives suggest

- (a) that metallic UHTMs have organised complexity,
- (b) that there is entanglement and
- (c) that the “affairs” of alloys cannot be separated from (are linked with)
  - (i) the “affairs” of phases and
  - (ii) the parameters that describe
    - (1) alloying behaviour and
    - (2) properties of alloys and phases, and
  - (iii) the (effects of the) environment (e.g., environmental degradation because of interstitial contamination, oxidation).

According to NICE, entanglement has profound implications for the design of metallic UHTMs (see below). The views of the “landscape” also hint at linkages of data that help one

- (d) to uncover
  - (iv) new things about alloys and their phases, things s/he might never have suspected, and
  - (v) regularities and linkages, and
- (e) to establish
  - (vi) relationships between different properties and
  - (vii) a framework of understanding that is subtle and mathematical.

Could the entanglement shown in the alloy design “landscape” in Figure 1 help the alloy designer to find unexpected new relationships as the range of investigated UHTMs is expanded? To answer this question, we must discover what else this “landscape” can divulge to us. Shall we walk together around the “landscape”? We must not forget to “open the door” of each bounded area to find what is kept inside (details about figures, relationships, maps and references).

### 5.1. Walk in the Superstructure of the “landscape”

Our walk starts at the entrance of the “landscape” on the left-hand side of Figure 1. We enter the first bounded area where we meet with the property targets (goals). The latter have been set by industry and are related to the requirement for new materials that would allow future aero engines to be more environmentally friendly and efficient [7–9,21].

We follow the solid green arrow and enter the second bounded area, which is on the right-hand side of the “landscape” entrance, where we see that the property targets are about the alloy steady-state creep rate ( $\dot{\epsilon}_{\text{alloy}}$ ), mass change ( $\Delta W_{\text{alloy}}$ ) in oxidation and yield strength ( $\sigma_y^{\text{alloy}}$ ). (A target for toughness has also been set by industry; this property is not included in NICE [7]). We find out that each one of the property targets correlates with alloy parameters that form the third bounded area in the “landscape” on the right-hand side of the second bounded area. The second and third bounded areas are linked with a solid green arrow. The steady-state creep rate  $\dot{\epsilon}_{\text{alloy}}$  links with  $\Delta X_{\text{alloy}}$ ,  $\text{VEC}_{\text{alloy}}$ , and  $\delta_{\text{alloy}}$ , shown with double dashed arrows, and examples of the correlations can be found, respectively, in the Figure 10a–c in [7]. The  $\Delta W_{\text{alloy}}$  links with  $\text{VEC}_{\text{alloy}}$  and  $\delta_{\text{alloy}}$ , shown with double dashed arrows, and examples of the correlations can be seen in the Figure 9 in [7], Figure 13a,c in [60] and Figure 15a in [46] for the former parameter, and in the Figure 13b,d in [60]

and the Figure 15b in [46] for the latter parameter. The  $\sigma_y^{\text{alloy}}$  links with  $\Delta\chi_{\text{alloy}}$ ,  $\text{VEC}_{\text{alloy}}$ , and  $\delta_{\text{alloy}}$ , shown with double dashed arrows, and examples of the correlations of alloy hardness and alloy specific yield strength can be found, respectively, in the Figure 11c in [21] and the Figure 18a in [48] for the first parameter, the Figure 11d in [21], the Figure 6 in [9], the Figure 19 in [48], the Figure 8a in [60] and the Figure 8d in [60] for the second parameter, and in the Figure 18b in [48] for the third parameter.

The aforementioned correlations/relationships indicate that one can use the value of a property goal to calculate the corresponding alloy parameter value from the relevant correlation. For example, for the creep rate goal, from  $\dot{\epsilon}_{\text{alloy}} = g_1(\Delta\chi_{\text{alloy}})$  we calculate  $\Delta\chi_{\text{alloy}}$ , from  $\dot{\epsilon}_{\text{alloy}} = f_1(\text{VEC}_{\text{alloy}})$  we calculate  $\text{VEC}_{\text{alloy}}$  and from  $\dot{\epsilon}_{\text{alloy}} = h_1(\delta_{\text{alloy}})$  we calculate  $\delta_{\text{alloy}}$ , where  $g_1$ ,  $f_1$  and  $h_1$  are mathematical functions. We also find out that the entanglement of alloy properties with alloy parameters has led to the discovery of relationships between the creep rate of a metallic UHTM with the ratios Nb/(Ti + Hf) and sd/sp, i.e., relationships of the form  $\dot{\epsilon}_{\text{alloy}} = g_2([\text{Nb}/(\text{Ti} + \text{Hf})]_{\text{alloy}})$ , e.g., see the Figure 19 in [7] and  $\dot{\epsilon}_{\text{alloy}} = g_3([\text{sd}/\text{sp}]_{\text{alloy}})$ , e.g., see the Figure 20 in [7].

As we wander inside the third bounded area, we discover that each alloy parameter correlates with the alloy's concentration C of solute X. In other words, we discover that there are relationships of the form  $C_X^{\text{alloy}} (\text{at.}\%) = p(P_{\text{alloy}})$ , where P is  $\Delta\chi_{\text{alloy}}$ ,  $\text{VEC}_{\text{alloy}}$  or  $\delta_{\text{alloy}}$  and p is a mathematical function. We find out examples (i) for  $C_X^{\text{alloy}} (\text{at.}\%) = p_1(\Delta\chi_{\text{alloy}})$  in the Figure 12a in [7], the Figure 10a in [19] and the Figure 9c,f,i in [60], (ii) for  $C_X^{\text{alloy}} (\text{at.}\%) = p_2(\text{VEC}_{\text{alloy}})$  in the Figure 12a in [7], Figure 18a in [21], Figure 10b in [19], Figure 9a,d,g in [60] and (iii) for  $C_X^{\text{alloy}} (\text{at.}\%) = p_3(\delta_{\text{alloy}})$  in the Figure 9b,e,h in [60]. Thus, we understand that the entanglement of property goals with alloy parameters empowers one to calculate the alloy chemical composition,  $C_{\text{alloy}}$ . There are cost issues regarding the elements that "make up the alloy", which (the costs) result from the availability and cost of specific raw materials, as well as recyclability and sustainability interests that must be addressed together with processability matters. We move from the third bounded area in the direction of the solid brown arrow in Figure 1. While we wander inside the third bounded area, we discover that the alloy parameters also work together, i.e., they are in synergy (shown with the double blue arrows in the third bounded area). We find correlations that result from the synergy of alloy parameters in the Figure 15b in [19], Figure 16 in [48], Figure 14 in [46], Figure 15a in [44], Figure 15 in [45], Figure 19 in [8], Figure 2 in [21] and the Figures 3 and 4 in [59].

We exit the third bounded area in the "landscape" and move in the direction of the solid green arrow to enter the fourth bounded area. This area is about the bcc solid solution in metallic UHTMs. Here, we encounter the parameters  $\Delta\chi_{\text{Nbss}}$ ,  $\text{VEC}_{\text{Nbss}}$  and  $\delta_{\text{Nbss}}$  of the bcc Nb solid solution. We discover that parameters of the alloy link with parameters of the solid solution, i.e., with relationships of the form  $P_{\text{alloy}} = q(P_{\text{Nbss}})$  where P is  $\Delta\chi$ , VEC or  $\delta$  and q is mathematical relationship. These links are shown with dashed arrows between the third and the fourth bounded areas. They are described with mathematical relationships such as (i)  $\Delta\chi_{\text{alloy}} = q_1(\Delta\chi_{\text{Nbss}})$ , examples of which are found in the Figures 3a and 6a in [20], (ii)  $\text{VEC}_{\text{alloy}} = q_2(\text{VEC}_{\text{Nbss}})$ , examples of which are shown in the Figure 17 in [7], Figure 17a in [21], Figure 3b in [20] and Figure 6a in [8] and (iii)  $\delta_{\text{alloy}} = q_3(\delta_{\text{Nbss}})$  (figures not published).

While we stroll inside the fourth bounded area, we discover that the entanglement of alloy, solid solution and parameters enables one to get the chemical composition of the solid solution. Indeed, we discover that the chemical composition of the solid solution can be calculated from relationships of the form  $P_{\text{Nbss}} = k(C_X^{\text{Nbss}})$  where P is  $\Delta\chi$ , VEC or  $\delta$ , k is mathematical relationship, and C is the concentration of element X in the solid solution. We find out examples (i) for  $\Delta\chi_{\text{Nbss}} = k_1(C_X^{\text{Nbss}})$  in the Figure 11a in [20] and Figure A1a,c in [60], (ii) for  $\text{VEC}_{\text{Nbss}} = k_2(C_X^{\text{Nbss}})$  in the Figure 11c in [20], Figure 18b in [21], and Figure 4d–f in [60], and (iii) for  $\delta_{\text{Nbss}} = k_3(C_X^{\text{Nbss}})$  in the Figures 7 and 11b in [20] and the Figure A1b in [60]. In other words, having entered the fourth bounded area and looked around it, we realise that the entanglement of property goals with alloy parameters  $P_{\text{alloy}}$  and solid solution parameters  $P_{\text{Nbss}}$ , where P is  $\Delta\chi$ , VEC or  $\delta$ , empowers one to calculate

the solid solution chemical composition  $C_{Nb_{ss}}$ . Thus, we move from the fourth bounded area in the direction of the solid red arrow in the Figure 1.

As we wander backwards and forwards between the brown box of  $C_{alloy}$ , the third and fourth bounded areas and the red box of  $C_{Nb_{ss}}$ , we discover that owing to the said entanglement, there is another way to calculate the chemical composition of the solid solution, namely from relationships of the form  $C_X^{alloy} = m(C_X^{ss})$  (shown with the thin red arrow in Figure 1), examples of which are shown in the Figure 16 in [7] and Figure 19b in [21], or from other relationships such as  $VEC_{alloy} = n(C_X^{Nb_{ss}})$ , an example of which is shown in the Figure 19a in [21]. Furthermore, we discover that the concentrations of solutes in the solid solution are linked (the link with solute relationships is also shown with a thin red arrow in Figure 1), examples of which are shown in the Figures 8 and 9 in [20], Figure 11 in [19], Figure 16 in [61], Figure 7 in [48], Figure 4a–c in [60], Figure 12d,e in [46] and relationships linking the concentrations of Ti with specific solutes, i.e.,  $Ti_{ss} = d_1(C_X^{ss})$  shown in the Figure S4 in supplemental data in [74], Figure 12a–c in [46], Figure 12 in [45], Figure 9 in [7] and the Figure 19c,d in [19]. While we are thinking about our next step in the “landscape”, we are excited to note that the said entanglement has directed research to find out that the solid solution, which in metallic UHTMs can be “normal”, Ti-rich or Si-free according to solute partitioning [55], can also be “conventional”, CC or HE [20] according to its chemical composition, and that the research has discovered relationships that link these solid solutions, for example see the  $\Delta\chi^{“conventional” Nb_{ss}} = b(\Delta\chi_{CC/HE Nb_{ss}})$  relationship in the Figure 6b in [20].

The fact that there are relationships between alloy parameters, the existence of which was realised when we strolled in the third bounded area, makes us wonder whether the solid solution parameters also work together, i.e., they are in synergy. Returning to the fourth bounded area, we discover this is the case (shown with the double blue arrows). Examples of correlations that result from the synergy of solid solution parameters are relationships such as  $VEC_{ss} = h_1(\delta_{ss})$ , shown in the Figure 10b in [20],  $VEC_{ss} = \psi_3(\Delta\chi_{ss})$ , shown in the Figures 6c and 10c in [20] and Figure 8c in [48],  $\Delta\chi_{ss} = h_3(\delta_{ss})$ , shown in Figure 10a in [20], and  $\delta_{ss} = h_4(\Delta H_{mix})_{ss}$  and  $\Omega_{ss} = m(\Delta H_{mix})_{ss}$ , shown in the Figure 8a,b in [48].

We return to the third bounded area in the “landscape”, move in the direction of the solid green arrow and enter the fifth bounded area, which is about the 5-3 silicide of Nb in metallic UHTMs. Here, we find the parameters  $\Delta\chi_{Nb_5Si_3}$  and  $VEC_{Nb_5Si_3}$  of the silicide. We discover that parameters of the alloy link with parameters of the 5-3 silicide with relationships of the form  $P_{alloy} = t(P_{Nb_5Si_3})$  where P is  $\Delta\chi$  or VEC and t is a mathematical relationship. These linkages are shown with dashed arrows between the third and fifth bounded areas. For  $VEC_{alloy} = t_1(VEC_{Nb_5Si_3})$ , examples are found in the Figure 6a in [58] and Figure 17b in [21] (figures for the relationship  $\Delta\chi_{alloy} = t_2(\Delta\chi_{Nb_5Si_3})$  have not been published). There is also a relationship between VEC and  $\Delta\chi$ , namely  $VEC_{alloy} = t_3(\Delta\chi_{Nb_5Si_3})$ , see Figure 7 in [21]. We discover that the chemical composition of the 5-3 silicide can be calculated from relationships of the form  $P_{Nb_5Si_3} = r(C_X^{Nb_5Si_3})$ , where P is  $\Delta\chi$  or VEC, r is mathematical relationship, and C is the concentration of element X in the silicide. For the relationship  $\Delta\chi_{Nb_5Si_3} = r_1(C_X^{Nb_5Si_3})$  examples are shown in the Figure 2b,c in [7] and Figure 5d in [60], and for  $VEC_{Nb_5Si_3} = r_2(C_X^{Nb_5Si_3})$  see the Figure 2a in [56], Figure 18c in [21] and the Figure 5c in [60].

In other words, having entered the fifth bounded area and looked around it, we realise that the entanglement of property goals with alloy parameters  $P_{alloy}$  and silicide parameters  $P_{Nb_5Si_3}$ , where P is  $\Delta\chi$  or VEC, allows one to calculate the silicide chemical composition  $C_{Nb_5Si_3}$ . We move from the fifth bounded area in the direction of the solid purple arrow in the Figure 1. We are excited to discover that concentrations of solutes in the silicide are linked, as was the case for the solid solution. We find examples of solute correlations in the Figure 11 in [19], Figures 12 and 13 in [61] and the Figure 13 in [45], examples of relationships linking the concentrations of Ti with specific solutes, i.e.,  $Ti_{Nb_5Si_3} = d_2(C_X^{Nb_5Si_3})$ , in the Figure 1b–d in [7], Figure 8a,b in [63] and the Figure 20 in [21] and examples of

relationships linking the concentrations of Nb and Hf, i.e.,  $Nb_{Nb_5Si_3} = d_3(Hf_{Nb_5Si_3})$ , in the Figure 1a in [7] and the Figure 8c in [63]. The link of the chemical composition of the silicide and solute relationships is shown also with a thin purple arrow in Figure 1.

We stand back and look again at the “landscape”. We discover that from the chemical composition  $C_{alloy}$  of an alloy, one can calculate macrosegregation (MACX) of elements and alloy properties via the aforementioned parameters (i.e., the relationships  $[Property]_{alloy} = f(P_{alloy})$ , where P is  $\Delta\chi$ , VEC or  $\delta$  discussed above) and other relationships, for example,  $HV_{alloy} = t_1((\Delta H_{mix})_{alloy})$  and  $HV_{alloy} = t_2((\Delta S_{mix})_{alloy})$ , as shown respectively in the Figure 11a,b in [21]. We also discover how properties depend on the volume fractions of phases, examples of which can be found in the relationships  $HV_{alloy}$  versus vol.%  $Nb_{ss}$  in the Figure 15e in [19],  $HV_{alloy}$  versus vol.% A15 in Figure 22c in [61],  $HV_{alloy}$  versus vol.%  $Nb_5Si_3$  in Figure 22d in [61] and  $[\Delta W/A]_{alloy}$  versus vol.%  $Nb_{ss}$  in Figure 16a in [19].

Furthermore, we find out that from the chemical composition of the bcc solid solution, we can calculate its strength via the aforementioned parameters, i.e., from relationships  $(\sigma_y)_{ss} = g(P_{ss})$ , where P is  $\Delta\chi$ , VEC or  $\delta$  and g is mathematical relationship (for examples see the relationships  $HV_{ss} = g_5(\Delta\chi_{ss})$  in the Figure 13c in [21],  $HV_{ss} = f(VEC_{ss})$  in the Figure 17 in [48] and the Figure 6a–c in [60] and  $HV_{ss} = h_2(\delta_{ss})$  in the Figure 7 in [8] and the Figure 4 in [9]) and other relationships, for example, the relationship  $HV_{ss}$  versus  $\Omega_{ss}$  shown in the Figure 13a in [20] and  $HV_{ss} = h(C\chi^{ss})$  shown in the Figure 7 in [60]. We also discover that the vol.% of the bcc solid solution is related to alloy parameters and the chemical composition of the solid solution, as shown with the relationships of vol.%  $Nb_{ss}$  versus  $VEC_{alloy}$  in the Figure 16c in [19], Figure 18a in [61], vol.%  $Nb_{ss}$  versus  $\Delta\chi_{alloy}$  in Figure 16b in [19] and Figure 22b in [61] and vol.%  $Nb_{ss}$  versus  $C_{ss}$  in Figure 9 in [46].

Moreover, we discover that from the chemical composition of the 5-3 silicide, we can calculate properties of the silicide from relationships like  $[Property]_{Nb_5Si_3} = g(P_{Nb_5Si_3})$ , where P is  $\Delta\chi$  or VEC, for example, see the relationship  $HV_{Nb_5Si_3} = f_7(VEC_{Nb_5Si_3})$  in the Figure 5 in [9]. Similarly, with the bcc solid solution, we also discover that the volume fraction of intermetallics is related to alloy parameters, as shown with the relationships linking the volume fractions of  $Nb_5Si_3$ , A15- $Nb_3X$  and C14- $NbCr_2$  Laves with  $VEC_{alloy}$  in the Figure 18b–d in [61].

## 5.2. Walk in the Substructure of the “Landscape”

A huge volume of data about alloys is generated worldwide. Researchers accumulate data and construct a worldview of what is going on. Alloy developers must (i) make sense of data relevant to metallic UHTMs and (ii) combine bits of data into a broad picture of these materials. Critical thinking, communication, collaboration, and creativity [8] would help the researchers to feed the latest knowledge in an alloy design “landscape”.

One could enter the “landscape” shown in Figure 1 from the latest knowledge side. Here, s/he will meet with the “substructure” of the “landscape”. Examples of latest knowledge that feed in the “landscape” are the extensive and continuous metallurgical and materials science research on HEAs, CCAs, RCCAs and RHEAs, e.g., [75–85], research on RMICs, e.g., [86–92], research on mechanical properties, oxidation, e.g., [86,93–103] and processing, e.g., [75,76,78,102], data relevant to phase equilibria and phase diagrams, e.g., [71,72,104–112], all of which is assessed and evaluated within and without NICE. However, the latest knowledge does not stop to the aforementioned but includes other types of knowledge, for example, knowledge generated from the pursuit of sustainability and sustainable development [113], from the concept of “circular economy” in the sustainability debate, and environmental risks, and linked with research about shortage of resources and recyclability, and with the exchange of ideas about and discussion of responsible research and innovation, e.g., [114–116]. In other words, the “landscape” in Figure 1 connects with other processes of knowledge production, the relationship between science, engineering and society, environmental degradation of materials, and is enthusiastic about knowledge transmission.

Indeed, NICE, via the new knowledge, links in the “landscape” with (a) phase equilibria, (b) environment/interstitial contamination, (c) properties of elements and phases, (d) raw materials, processing and ecological costs/issues, and (e) risks, and with its typical characteristics/features of synergy, entanglement and self-regulation (see below) can deal with change, to constantly learn new things and stay relevant. The latest knowledge in the “landscape” meets with the new knowledge created with NICE within the “landscape”. For example, new knowledge can be about the effects of exposure to different environments on mechanical properties (e.g., stress rupture life, fatigue crack propagation) and oxidation (isothermal and cyclic) of metallic UHTMs and about (a) phase equilibria and phase transformations, (b) processing, (c) properties. Let us expand on (a) to (c) in the next three paragraphs.

Regarding phase equilibria and phase transformations, examples are

- (1) the clarification of three phase equilibria between  $Nb_{ss}$ ,  $Nb_5Si_3$  and  $C14-NbCr_2$  in the Nb-Si-Cr ternary [38],
- (2) studies of phase equilibria in the Nb-Ge-Si [39] and Nb-Al-Sn [40] ternary systems (Al, Cr, Ge, Si and Sn are key solute additions in metallic UHTMs for oxidation resistance [7,8]),
- (3) precipitation of  $Nb_{ss}$  in  $Nb_5Si_3$  in heat-treated alloys, see data for the alloys KZ7 (Nb-24Ti-18Si-5Al, [117,118]), JG1 (Nb-18Si-5Al-5Cr-5Mo, [119]), KZ5 (Nb-24Ti-18Si-5Al-5Cr), KZ6 (Nb-24Ti-18Si-5Al-5Cr-6Ta), KZ2 (Nb-24Ti-18Si-4Al-8Cr), KZ8 (Nb-24Ti-18Si-4Al-8Cr-6Ta) [118], ZF8 (Nb-18Si-5Al-5Ge) and ZF5 (Nb-24Ti-18Si-5Al-5Ge) [120] and the alloy CM1 (Nb-8Ti-21Si-5Mo-4W-1Hf) [74] (in the parentheses are given the nominal compositions, at.%),
- (4) precipitation of  $A15-Nb_3X$  in heat-treated alloys, see data for the alloys EZ5 (Nb-24Ti-18Si-5Al-5Hf-5Sn), EZ8 (Nb-24Ti-18Si-5Al-5Cr-5Hf-5Sn) [61], ZX4 (Nb-24Ti-18Si-5Cr-5Sn), ZX6 (Nb-24Ti-18Si-5Al-5Sn) [42] and JG6 (Nb-24Ti-18Si-5Al-5Cr-5Hf-2Mo-5Sn) [121] (note that in JG6-HT the Sn rich Nb<sub>ss</sub> that was reported in [121] subsequently was confirmed to be the A15 compound),
- (5) precipitation of  $Nb_{ss}$  and/or  $A15-Nb_3X$  in heat treated alloys, see data for the alloys NV8 (Nb-24Ti-18Si-5Fe-5Sn) [122], NV5 (Nb-24Ti-18Si-5Cr-5Fe-5Sn) [123], JZ4 (Nb-11.5Ti-18Si-5Mo-2W-4.9Sn-4.6Ge-4.5Cr-4.7Al-1Hf), JZ5 (Nb-21Ti-18Si-6.7Mo-1.2W-4.4Sn-4.2Ge-4Cr-3.7Al-0.8Hf) [46], JZ3 (Nb-12.4Ti-17.7Si-6Ta-2.7W-3.7Sn-4.8Ge-4.7Al-5.2Cr-1Hf). JZ3+ (Nb-12.4Ti-19.7Si-5.7Ta-2.3W-5.7Sn-4.9Ge-4.6Al-5.2Cr-0.8Hf) [45], EZ4 (Nb-18Si-5Al-5Hf-5Sn) [62], ZX5 (Nb-24Ti-18Si-5Al-2Sn) and ZX7 (Nb-24Ti-18Si-5Al-5Cr-2Sn) [41],
- (6) stability of  $A15-Nb_3X$ ,  $C14-NbCr_2$ , tP32  $Nb_3Si$ , metastable  $Nb_3Si$  [19,61,62],
- (7) phase equilibria between “conventional” and CC/HE  $Nb_{ss}$  and  $Nb_5Si_3$  [9,19,20,48,61],
- (8) phase transformations associated with CC/HE phases [61],
- (9) relationships between solutes in hexagonal  $D8_8$  5-3 silicide in B containing RCCAs [48],
- (10) effects of different solute additions on the chemical composition of eutectics with  $Nb_{ss}$  and  $Nb_5Si_3$  [61], and
- (11) solubility range of
  - (i) X in  $A15-Nb_3X$  (X = Al, Ge, Si, Sn) [42,61],
  - (ii)  $\langle Si \rangle$  in  $Nb_5\langle Si \rangle_3$  ( $\langle Si \rangle$  = Al, Ge, Si, Sn) [56], and
  - (iii)  $\langle Si \rangle$  in tetragonal  $D8_1$  (T2) and hexagonal  $D8_8$  5-3 silicide in B containing RCCAs ( $\langle Si \rangle$  = Al, B, Si, Sn) [48].

In relation to processing, examples include

- (12) the effects of processing and alloy chemical composition on the type of  $Nb_5Si_3$  in metallic UHTMs [62],
- (13) subgrain formation in  $Nb_5Si_3$  is cast and OFZ (optical floating zone) grown alloy CM1 (Nb-8Ti-21Si-5Mo-4W-1Hf) [74], and
- (14) effect of processing on macro and micro-segregation [8,74].

With regard to properties, examples can be found vis-à-vis



- (15) alloy oxidation, which improves with the addition of Ge and/or Sn that segregate to the surface where
  - (i) Sn-rich areas are formed, and Sn-containing compounds precipitate and
  - (ii)  $\text{Nb}_5(\text{Si,Ge})_3$  is formed [28,41–47],
- (16) correlations of the hardness
  - (iii) of the bcc solid solution with  $\delta_{\text{ss}}$ ,  $[\text{O}_{\text{ss}}]$  [8,9,20], and  $\Omega_{\text{ss}}$ ,  $(\Delta H_{\text{mix}})_{\text{ss}}$ ,  $(\Delta S_{\text{mix}})_{\text{ss}}$  [21],
  - (iv) of  $\text{Nb}_5\text{Si}_3$  with solutes [56] and with  $\text{VEC}_{\text{Nb}_5\text{Si}_3}$  [9,21,58],
  - (v) of alloys with  $\text{VEC}_{\text{alloy}}$ ,  $\Delta\chi_{\text{alloy}}$ ,  $(\Delta H_{\text{mix}})_{\text{alloy}}$ ,  $(\Delta S_{\text{mix}})_{\text{alloy}}$  [21],
- (17) relationship of specific strength with  $\text{VEC}_{\text{alloy}}$  [8,9],
- (18) correlations of the Young's moduli of the bcc solid solution with the concentration of oxygen owing to interstitial contamination [20],
- (19) relationships between the hardness of eutectics with  $\text{Nb}_{\text{ss}}$  and  $\text{Nb}_5\text{Si}_3$  with the parameters  $\text{VEC}_{\text{eutectic}}$  [57],  $\delta_{\text{eutectic}}$  and  $\Delta\chi_{\text{eutectic}}$  [21],
- (20) correlations of the steady-state creep of  $\text{Nb}_5\text{Si}_3$  with the parameters  $\text{VEC}_{\text{Nb}_5\text{Si}_3}$ ,  $\delta_{\text{Nb}_5\text{Si}_3}$  and  $\Delta\chi_{\text{Nb}_5\text{Si}_3}$  [9],
- (21) relationships of the parameters  $\text{VEC}_{\text{ss}}$ ,  $\delta_{\text{ss}}$  and  $\Delta\chi_{\text{ss}}$  with the concentration of oxygen in the bcc solid solution owing to its interstitial contamination [20],
- (22) correlations about the contributions of solute elements to the steady state creep of the alloy [21] and
- (23) creep map for alloys [9].

In the “substructure” of the “landscape”, we find out that atomic size, electronegativity, and valence electrons “support” the “landscape” with their correlations with the diffusivity and elastic properties of elements that are components of metallic UHTM, and with their correlations with the elastic properties of 5-3 silicides. We find examples of these correlations in the Figures 1–4 in [55], Figures 1, 2, 3a and 8 in [7] and in the Figure 1 in [21] for the elements, and in the Figure 3b to d and the Figure 4 in [7] and the Figure 14 in [8] for the silicides. We discover that in these correlations, (a) the elements belong in distinct groups and that these groups are associated with the distinct locations that metallic UHTMs have in alloy maps based on alloy parameters, as corroborated by the Figures 1–5 in [59], the Figure 19 in [8], the Figures 2 and 5 in [21], the Figures 1 and 2 in [9], and (b) the silicides also form distinct groups in silicide maps based on silicide parameters, depending on the solutes that substitute Si or Nb, as confirmed by the Figures 5–11 in [56], the Figure 6 in [21], the Figure 3e in [9], and the Figures 1e, 2e, 3e and 4e in [58].

The importance of the environment comes into view in the “landscape” in Figure 1, using as an example the interstitial contamination box in the groundwork of the “landscape”, and indicates the significance of metallic UHTM-environment “interaction”. Interstitial contamination is key for the design, processing and properties of metallic UHTMs with/without the addition of reactive elements like Hf, Ti or Zr, owing to the sensitivity of RMs to interstitial contamination [8] and the effect that such contamination has on phase equilibria, e.g., [19,124–132] and stability of microstructures [133]. The interstitial contamination (a) links with properties, e.g., [134–154], (b) with diffusivities, e.g., [155–160], (c) with solutes that slow down diffusivity of oxygen, e.g., references [43,161–163] and the Figure 17 in [19], and (d) with elastic properties of intermetallics contaminated with oxygen, e.g., [164–166]. Interstitial contamination affects the hardness and Young's modulus of the bcc  $\text{Nb}_{\text{ss}}$  solution and  $\text{Nb}_5\text{Si}_3$  [20,167,168]. Furthermore, the interstitial contamination of the bcc solid solution, 5-3 silicide, and A15 compounds differ, depending on solute elements in each phase and is more severe for the solid solution, e.g., Figure 17 in [19], and the severity of contamination of the aforementioned phases depends on location in the metallic UHTM, e.g., see the Figure 12c in [20]. Moreover, the parameters  $\Delta\chi$ ,  $\delta$  and  $\text{VEC}$ , the hardness and Young's modulus of the bcc solid solution increase with increasing contamination with oxygen; see Figures 11, 12d, 14c and 16 in [20]. Likewise, the parameters and properties of the 5-3 silicide depend on interstitial contamination.

## 6. Self-Regulation

NICE (a) has corroborated that it is possible to design alloys to meet the creep goal [8], (b) drew attention to the fact that one can get close to meeting the oxidation goal, (c) apprised the alloy designer about the importance of metallic UHTM-environment interactions, and (d) has warned the alloy developer (i) that it is unrealistic to aim to design metallic UHTMs to simultaneously meet creep and oxidation property targets in the same material and (ii) that the development of substrate metallic alloys must proceed hand in hand with the development of environmental coating systems, for which NICE can assist with the design of bond coat materials [9,64,68,69]. (In other words, NICE advises that we should aim to develop a materials system comprising of substrate plus environmental coatings for the “beyond the nickel-based superalloys era”). As a result, alloy designers must “fine-tune” their response to strategic priorities and design stimuli (incentives) that motivate the development of new metallic UHTMs, and either aim to design alloys with a balance of properties or aim to meet the goal (target) for a specific property. To put it another way, because of synergy and entanglement, an internal adaptive mechanism in NICE assists the alloy designer in meeting strategic priorities. I refer to this capability of NICE as self-regulation. Therefore, the features of the alloy design “landscape” drawn with NICE and shown in Figure 1 are synergy, entanglement, and self-regulation.

## 7. Synergistic Metallurgy

With CEMI (see Section 3), we can look at the principles of a material system and its evolution, both in service and as a design concept. For example, in the context of materials for high-pressure turbine applications in a gas turbine engine, a material system comprises a metallic UHTM substrate plus an environmental coating. The latter could be of the bond coat/thermally grown oxide/topcoat, with a layered multi-material or a functionally graded material as its bond coat. I used the word evolution because, in my opinion, alloy design ought to be able to deal with modes of change of a material or a material system, directional change or cumulative change and also because I wish to emphasize the importance of the cultural realm for the development of materials and material systems.

NICE makes it possible to deal both with material systems and their evolution. The material system necessitates understanding the processes via which its different interconnected parts justify their aggregate (holistic) identity. The interconnected parts are entangled and in synergy. Evolution in service ensues, for example, from interactions of the whole system with the environment, from inter-diffusion between the substrate and bond coat, between the layered components of the multi-material bond coat or from phase transformations in a functionally graded bond coat, some of which might be triggered by interstitial contamination. This evolution, as a way that produces change, could generate a variety of microstructures, some of which may be attributed to changes in phase equilibria and bring about changes in mechanical and thermo-physical properties of the material system. The above feed in NICE, meaning new knowledge generated via the design methodology (Figure 1), and, for example, facilitate the design of new material systems, the modification of existing ones, points to changes in manufacturing procedures or hint at new experiments. Thus, the correlative environment material interaction (CEMI) produces changes interrelated with prolonging the use of the material system in service. I wish to call this “evolution through survival” (ETS). In other words, the arising/resulting changes shape something akin to an environmental system. CEMI, ETS and IRIS are in synergy supported by and backing ESSERE (see Section 3 and Appendix A) (Figure 2).

I “define” synergistic metallurgy the metallurgy depicted in the Figure 1 (and its extension for alloys with three or more phases, see Section 5) and Figure 2. The synergistic metallurgy, in partnership/alliance with chemical, mechanical, physical and process metallurgy, works together with the science and engineering disciplines and has the capacity to affect the development of how materials (i) are developed, produced and used and

(ii) change the world. Synergistic metallurgy invokes probabilistic dealing with a situation or problem, what is likely to happen, what could happen, and what tends to happen.

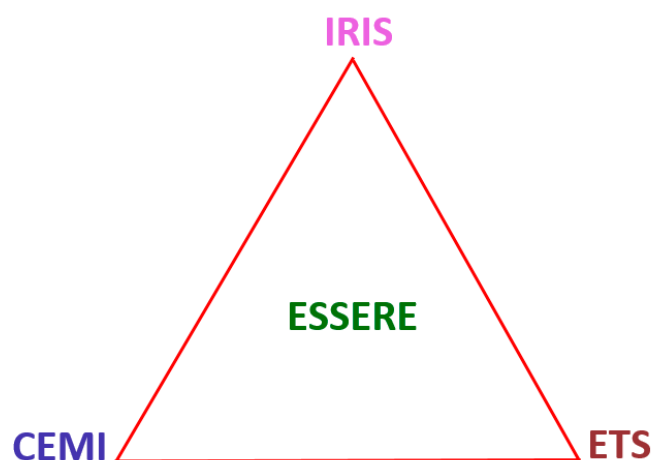


**Figure 2.** A schematic diagram showing the link between CEMI, ETS, IRIS and ESSERE. For the links of this figure with NICE, see the text.

### 8. Afterword

Let us reflect on what we have seen and learned from our “walk” in the alloy design “landscape”. In our “walk”, we viewed the parts that make up the “landscape” as distinct groups, but they are entangled. The NICE methodology seeks to broaden our horizons, open new and unknown futures, make us aware of possibilities we do not normally consider and emphasizes the key role of the environment-material interactions in the design and development of metallic UHTMs.

Synergy and entanglement demonstrated how relationships between parameters of alloys and their phases, between the same parameters and properties of alloys and their phases, shape a subtle and harmonious methodology to process alloy design/selection through a progressive goal-oriented approach. What we need to know is not simply where we are going but also where we are and where we can go. We should be aware of “path dependence”, meaning that the order in which decisions are taken affects their outcome.

The available data gives a realistic (workable, consistent) account of how the alloying behaviour and properties of alloys and their phases are “determined (controlled)” by different groups of elements working together and with the environment in a metallic UHTM. In the latter, different elements with similar or different concentrations and different levels of structure (meaning the different or similar structures of elements and of the phases such as solid solution(s) and intermetallic(s) that make up the alloy microstructure with a particular “architecture” (e.g., co-continuous solid solution(s)-intermetallic(s)) that are influenced by internal processes (e.g., solute partitioning) or the environment (e.g., contamination with interstitials) in which the alloy is produced and/or operates, are in synergy. Partitioning of solutes can result (i) in a change in the crystal structure (e.g., the case of Ti partitioning to  $Nb_5Si_3$  and substituting Nb, thus causing a change in structure from tetragonal to hexagonal as well as changes in mechanical properties [27]) or (ii) to the formation of sub-grains in  $Nb_5Si_3$  [74] while change in structure also can occur with contamination with interstitials (for example, the case of hexagonal instead of tetragonal  $Nb_5Si_3$  stabilised in Nb-Si alloys with C contamination [169]).

Underlying the complexity of metallic UHTMs is the apparent simplicity of relationships that enable organised complexity to emerge by means of synergy and entanglement. The organizational properties of these complex alloys are attributed to the relationships of parameters that reflect the specific nature of the alloys concerned. Regularities have contingent features, meaning they depend upon something beyond themselves, for example,

contamination by interstitials owing to interaction with the environment [20,169], and thus, parameter values and relationships change.

The building blocks in the “landscape” in the Figure 1 were not “given”. They had to be created. The “landscape” created with NICE reflects a complex interaction between change and strategic innovation. Alloy design requirements change in response to the needs of innovations achieved (gained) by strategy. Uncertainty is intrinsic in the design of metallic UHTMs. Its significance is that it turns planning for the future into an ongoing learning proposition.

A characteristic feature of the “landscape” is that its parts interact in many ways. Collective properties result from the properties of the parts, and behaviour at a larger scale results from the detailed structure and relationships at a finer scale. In other words, as we walked in the “landscape”, we moved across different length scales. From the “landscape”, we can find out what could happen to the alloy (material system) on account of its relationship with its environment. The “landscape” suggests (hints, implies) that properties that we associate with an alloy (material system) are dependent on the relationship between parts of the material system and its environment.

Thanks to synergy, information about alloy (material system) behaviour and properties can be extracted owing to the coexistence of phases and phase types and the resourcefulness of parameters; the information cannot be obtained from the individual parts considered individually.

Synergy and entanglement are mutually affecting. There is a constant interaction between the two. The link between them is not merely causal but relational. They are not made in relationships. They are made of relationships. The dynamic interplay between synergy, entanglement, self-regulation and the reasonable (and acceptable) goals of industry must be satisfied before we can say that the development of an alloy has been achieved. The balance of properties is a dynamic situation maintained and adjusted by synergy and entanglement.

Implicit in the alloy design “landscape” is the idea of self-regulation. Alloy development is bound by norms and must agree to limit itself according to the norms it serves. Alloy development rules are normative (set a standard). The normative power of an alloy development rule depends on its thought-provoking (motivating) power. (NICE via the parameters VEC,  $\Delta\chi$  and  $\delta$  warns the alloy designer that the key property goals for metallic UHTMs conflict, for example, the parameters VEC and  $\delta$ , and the alloying with Boron “limit” what the alloy designer can do for oxidation versus creep [7–9], and the parameters VEC and  $\Delta\chi$  for the creep of  $\text{Nb}_5\text{Si}_3$  [56]).

Metallic UHTMs must be understood holistically, and the properties of a metallic UHTM are comprehended by studying the alloying behaviour and properties of its constituent phases. Synergy and entanglement plus self-regulation point to alloy development using both reductionist and holistic approaches.

The latest scientific, technological, and institutional knowledge and know-how can come from any part of the world, as R&D is not the monopoly of any country. Resulting knowledge and know-how relevant to metallic UHTMs will feed in NICE and the alloy design “landscape”. If a single country or research community were to pursue a high-risk, high-gain technology path, other countries and research communities would most likely be forced to do the same and “fomo” (see Abbreviations) becomes effective (“kicks in”). Research outcomes relevant to metallic UHTMs will feed in NICE and the alloy design “landscape”. New and latest knowledge relevant to metallic UHTMs produced respectively within and without NICE is likely to reinforce and compound one another. In other words, the connectivity (within and without the “landscape”) and updateability of NICE demonstrated that the “landscape” embodies evolutionary rationality.

Risks and ecological challenges arising from the development of metallic UHTMs, e.g., risks associated with (i) potential need for strategic low availability alloying elements, (ii) scale-up [8], (iii) uncertainty about metallic UHTM capability and capability robustness, (iv) high costs for material qualification, and (v) availability and applicability of probabilistic

methods to support alloy qualification and sustainability and recyclability can be managed with IRIS, CEMI, ETS and ESSERE. Material-environment interactions can be handled with CEMI (Sections 3 and 6). Recovery and/or recycling of scarce raw materials could accelerate the development of new technologies, affecting processability, component manufacture and microstructure architectures. The need for environmental coatings that protect metallic UHTM substrates from interstitial contamination could also lead to the development of new surface engineering technologies for the deposition of multi-material systems with tailor-made functionality for the bond coat and topcoat.

In the Table 1 is condensed the above discussion and the conclusions of this paper. The three attributes of NICE, namely synergy, entanglement, and self-regulation, enable the alloy designer to calculate the composition and properties of a metallic UHTM or a material system and its phases and link alloy design with costs, energy, processing and raw materials as well as with risk, sustainability, recyclability and material-environment interaction matters/concerns, which are dealt with the affiliates IRIS, CEMI, ETS and ESSERE.

**Table 1.** A summary perspective of the attributes and capabilities of NICE for the design and development of metallic UHTMs.

Attributes		Composition	Properties	Links with **		Affiliates +	
N I C E	Synergy	Metallic UHTM	Metallic UHTM	Costs	Risks	IRIS	E
	Entanglement	Material System *	Material System	Energy	Sustainability	CEMI	S
	Self-regulation	Phases	Phases	Processing	Recyclability	ETS	E
				Raw materials	Environment		R
						E	

\* see Section 7, + see Sections 3 and 7, \*\* see Sections 1 and 5.2.

## 9. Something to Think about

Have we considered including the environment-metallic UHTM interaction in our studies and models of mechanical properties, e.g., yield strength and creep, of an alloy and its phases? For example, we know that contamination with oxygen increases the yield strength and Young's modulus of Nb solid solution [20] and decreases the yield strength and Young's modulus of the Nb<sub>5</sub>Si<sub>3</sub> silicide [167,168], that contamination of the solid solution is more severe than that of the silicide [167,168], and that the contamination of each phase depends on how close the phase is to the scale/substrate interface and on the solute elements in the alloy and phases [19,20,167,168].

Have we considered modelling mechanical properties, e.g., creep, of metallic UHTMs with microstructures where “conventional” and CC/HE phases with/without interstitial contamination, namely bcc solid solutions and intermetallics, coexist [19,20]?

We might want to consider how to incorporate phase transformations, e.g., the precipitation of solid solution particles in intermetallics, in our models of mechanical properties, e.g., when we model the creep and/or toughness of metallic UHTMs.

It may be a good idea to take into account the changing (i.e., the dynamic) nature of the interfaces of M<sub>5</sub>Si<sub>3</sub> silicides with bcc solid solution(s) and/or other intermetallics, owing to the partitioning of solutes, contamination with interstitials and phase transformations of the silicide (e.g., see [45,61,62,74]) on mechanical behaviour at elevated temperatures.

In directionally solidified (DS) metallic UHTMs, macrosegregation profiles of elements depend on the overall alloy chemistry (meaning the elements that are in synergy in the alloy) and on growth rate [8,74,170]. Have we thought about manufacturing DS “composite” metallic UHTM components consisting of a core alloy surrounded by different (outer) alloy(s) and even using interstitial contamination of outer alloy(s) to modify and/or customise microstructure and properties?

We might want to think about how to additively manufacture metallic UHTM components with microstructures consisting of “conventional” and CC/HE phases with/without

metastable phases either in a layered structure with different functionalities for specific layers or as a concentric structure.

**Funding:** This research was supported by the University of Sheffield, Rolls-Royce Plc and EPSRC (EP/H500405/1, EP/L026678/1).

**Acknowledgments:** The support of this work by the University of Sheffield, Rolls-Royce Plc and EPSRC (EP/H500405/1, EP/L026678/1) is gratefully acknowledged. Discussions with all past and current members of the research group are gratefully acknowledged. For open access, the author has applied a 'Creative Commons Attribution (CC BY) licence to any Author Accepted Manuscript version arising.

**Conflicts of Interest:** The author declares no conflict of interest.

### Abbreviations

CALPHAD	Calculation of Phase Diagrams
CC	complex concentrated (also compositionally complex)
FOMO	fear of missing out
HE	high entropy
HV	hardness Vickers
MACX	macrosegregation of element X
NICE	Niobium Intermetallic Composite Elaboration
RM	refractory metal
RMIC	refractory metal intermetallic composite
RHEA	refractory metal high entropy alloy
RCCA	refractory metal complex concentrated alloy
RMIC/RHEA	RMIC that also meets the definition of RHEA
RM(Nb)IC	refractory metal intermetallic composite based on Nb
RM(Nb)IC/RCCA	RM(Nb)IC that also meets the definition of RCCA
RM(Nb)IC/RHEA	RM(Nb)IC that also meets the definition of RHEA
TM	transition metal
UHTM	ultra-high temperature material

### Appendix A. Clarifications/“Definitions”

Citizen *	Person (see below)
Culture *	the way of life of a particular society. For example, the people (persons, see <i>πρόσωπον</i> below) that lived in the ancient poleis (cities) of Athens and Sparta, i.e., the societies of Athens and Sparta, had different cultures (see polis below)
Ecclesia *	public legislative assembly of citizens that put citizen participation at its very core and underpinned the growth of a polis.
Entanglement	occurs when the (alloying) behaviour and properties (e.g., mechanical, environmental, thermo-physical) of a complex whole (alloy) cannot be described and understood independently from the behaviour of its parts (phases)
Essere	to be and to exist (verb in Vulgar Latin)
Intricateness	having many complexly interrelated parts (from <i>intricate</i> from Latin <i>intricatus</i> , which means entangled)
Inter-subjective	opinion exists within a communication network and links the subjective opinions of many individuals. Communication network is the structure and flow of communication and information between individuals within a group [171].

Landscape	Land + scape, scape from Old English sceppan or scyppan, meaning to shape (e.g., landscape is human-made space on the land or an area of the Earth's surface seen by an observer)
Methodology	derived from the words method and logos, method from μέθοδος, which derives from the verb μετέρχομαι that means movement for some purpose, and logos from λόγος, which derives from the verb λέγω that means tell, say
Polis *	City (here the word polis is used to describe the poleis (plural of polis) in ancient (classical age) Greece; see culture above)
Person *	πρόσωπον in Greek. The word πρόσωπον is made up of the preposition προς (=towards) and the noun ωψ (ωπός in the genitive), which means face, thus the composite word προς-ωπον. A person (πρόσωπον) has their face towards someone or something, s/he is opposite someone or something [53]
Synergy *	is derived from the Greek word συνεργία, which comes from syn/συν (=together) and ergon/έργον (=work), thus synergy = work together.
Topography	from topos/τόπος (=place) + graphy/γραφή (γραφή from γράφω = write about), or description of place

\* Relevant to Sections 3 and 4.

## Appendix B. Partitioning of Solutes

In boron-free RM(Nb)ICs, RM(Nb)ICs/RCCAs and RM(Nb)ICs/RHEAs, the partitioning behaviour of TMs, RMs and simple metal and metalloid elements affects the concentrations of Al, Cr, Mo, Si, Ta, Ti and W in the bcc solid solution and the 5-3 silicide. In the bcc Nb solid solution the concentration of Ti depends on the concentrations of RMs; it decreases as the RM content increases and vice versa, e.g., [45,46,74]. The increase in Ti concentration results in higher Cr and/or Al contents [117,118,172]. The concentration of Si can be zero (according to EPMA data) with specific RMs in solid solution, for example, with W [173] or with Mo and W or Ta [46,173,174], but not with Ta or Ta and W [45,118,174]. In alloys with Hf and Ti additions, the concentration of Hf in the Nb<sub>5</sub>Si<sub>3</sub> increases with increasing Ti content, and the Nb/(Ti+Hf) ratio decreases [45,46,61,63,65,73].

## References

- Cahn, R.W. Alloy design: A historical perspective. *Proc. Indian. Acad. Sci. Eng. Sci.* **1980**, *3*, 255–260. [CrossRef]
- Howe, A.; Farrugia, D. Alloy design: From composition to through process models. *Mater. Sci. Technol.* **1999**, *15*, 15–21. [CrossRef]
- Aeronautical Materials for Today and Tomorrow*; Forum organised by the Air and Space Academy (AAE), French Aerospace Society (3AF) and Academy of Technologies; SAGEM: Paris, France, 2012; ISBN 978-2-913331-56-3/979-10-92518-09-2.
- Bewlay, B.P.; Jackson, M.R.; Gigliotti, M.F.X. Chapter 6: Niobium silicide high temperature in situ composites. In *Intermetallic Compounds—Principles and Practice: Progress*; Wiley: Hoboken, NJ, USA, 2002; Volume 3, pp. 541–560.
- Heilmaier, M.; Krüger, M.; Saage, H.; Rösler, J.; Mukherji, D.; Glatzel, U.; Völkl, R.; Hüttner, R.; Eggeler, G.; Somsen, C.; et al. Metallic materials for structural applications beyond nickel-based superalloys. *JOM* **2009**, *61*, 61–67. [CrossRef]
- Tsakiroopoulos, P. Beyond Nickel Based Superalloys. In *Encyclopedia of Aerospace Engineering*; Wiley: Hoboken, NJ, USA, 2010. [CrossRef]
- Tsakiroopoulos, P. On Nb Silicide Based Alloys: Alloy Design and Selection. *Materials* **2018**, *11*, 844. [CrossRef]
- Tsakiroopoulos, P. Alloys for application at ultra-high temperatures: Nb-silicide in situ composites. *Prog. Mater. Sci.* **2022**, *123*, 100714. [CrossRef]
- Tsakiroopoulos, P. Refractory Metal Intermetallic Composites, High-Entropy Alloys, and Complex Concentrated Alloys: A Route to Selecting Substrate Alloys and Bond Coat Alloys for Environmental Coatings. *Materials* **2022**, *15*, 2832. [CrossRef] [PubMed]
- Senkov, O.N.; Tsakiroopoulos, P.; Couzinié, J.-P. Special Issue “Advanced Refractory Alloys”: Metals, MDPI. *Metals* **2022**, *12*, 333. [CrossRef]
- Cantor, B.; Chang, I.T.H.; Knight, P.; Vincent, A.J.B. Microstructural development in equiatomic multicomponent alloys. *Mater. Sci. Eng. A* **2004**, *375–377*, 213–218. [CrossRef]
- Tsai, M.-H.; Yeh, J.-W. High-Entropy Alloys: A Critical Review. *Mater. Res. Lett.* **2014**, *2*, 107–123. [CrossRef]
- Wei, X.; Olson, G.B. Integrated computational materials design for high-performance alloys. *MRS Bull.* **2015**, *40*, 1035–1044.
- Deschamps, A.; Tancret, F.; Benrabah, I.-E.; De Geuser, F.; Van Landeghem, H.P. Combinatorial approaches for the design of metallic alloys. *Comptes Rendus Phys.* **2018**, *19*, 737–754. [CrossRef]

15. Hafner, J.; Wolverton, C.; Ceder, G. Toward Computational Materials Design: The Impact of Density Functional Theory on Materials Research. *MRS Bull.* **2006**, *31*, 659–668. [[CrossRef](#)]
16. Wang, W.Y.; Li, J.; Liu, W.; Liu, Z.-K. Integrated computational materials engineering for advanced materials: A brief review. *Comput. Mater. Sci.* **2019**, *158*, 42–48. [[CrossRef](#)]
17. Okamoto, H. *Desk Handbook: Phase Diagrams for Binary Alloys*; ASM International: Metals Park, OH, USA, 2000.
18. Lukas, H.L.; Fries, S.G.; Sundman, B. *Computational Thermodynamics: The Calphad Method*; Cambridge University Press: Cambridge, UK, 2007.
19. Vellios, N.; Tsakiroopoulos, P. The Effect of Fe Addition in the RM(Nb)IC Alloy Nb–30Ti–10Si–2Al–5Cr–3Fe–5Sn–2Hf (at.%) on Its Microstructure, Complex Concentrated and High Entropy Phases, Pest Oxidation, Strength and Contamination with Oxygen, and a Comparison with Other RM(Nb)ICs, Refractory Complex Concentrated Alloys (RCCAs) and Refractory High Entropy Alloys (RHEAs). *Materials* **2022**, *15*, 5815. [[CrossRef](#)] [[PubMed](#)]
20. Tsakiroopoulos, P. On the Stability of Complex Concentrated (CC)/High Entropy (HE) Solid Solutions and the Contamination with Oxygen of Solid Solutions in Refractory Metal Intermetallic Composites (RM(Nb)ICs) and Refractory Complex Concentrated Alloys (RCCAs). *Materials* **2022**, *15*, 8479. [[CrossRef](#)]
21. Tsakiroopoulos, P. Refractory Metal (Nb) Intermetallic Composites, High Entropy Alloys, Complex Concentrated Alloys and the Alloy Design Methodology NICE—Mise-en-scène<sup>†</sup> Patterns of Thought and Progress. *Materials* **2021**, *14*, 989. [[CrossRef](#)] [[PubMed](#)]
22. Papadimitriou, I.; Utton, C.; Scott, A.; Tsakiroopoulos, P. Ab Initio study of the intermetallics in Nb–Si binary system. *Intermetallics* **2014**, *54*, 125–132. [[CrossRef](#)]
23. Papadimitriou, I.; Utton, C.; Tsakiroopoulos, P. Ab Initio investigation of the intermetallics in the Nb–Sn binary system. *Acta Mater.* **2015**, *86*, 23–33. [[CrossRef](#)]
24. Papadimitriou, I.; Utton, C.; Tsakiroopoulos, P. Ab Initio investigation of the Nb–Al system. *Comput. Mater. Sci.* **2015**, *107*, 116–121. [[CrossRef](#)]
25. Papadimitriou, I.; Utton, C.; Scott, A.; Tsakiroopoulos, P. Ab Initio study of binary and ternary Nb<sub>3</sub>(X,Y) A<sub>15</sub> intermetallic phases (X,Y = Al, Ge, Si, Sn). *Metall. Mater. Trans. A* **2015**, *46*, 566–576. [[CrossRef](#)]
26. Papadimitriou, I.; Utton, C.; Tsakiroopoulos, P. On the Nb–Ge binary system. *Metall. Mater. Trans. A* **2015**, *46*, 5526–5536. [[CrossRef](#)]
27. Papadimitriou, I.; Utton, C.; Tsakiroopoulos, P. The impact of Ti and temperature on the stability of Nb<sub>5</sub>Si<sub>3</sub> phases: A first-principles study. *Sci. Technol. Adv. Mater.* **2017**, *18*, 467–479. [[CrossRef](#)]
28. Papadimitriou, I.; Utton, C.; Tsakiroopoulos, P. Ab Initio Study of Ternary W<sub>5</sub>Si<sub>3</sub> Type TM<sub>5</sub>Sn<sub>2</sub>X Compounds (TM = Nb, Ti and X = Al, Si). *Materials* **2019**, *12*, 3217. [[CrossRef](#)] [[PubMed](#)]
29. Abel, M.-L.; Tsakiroopoulos, P.; Watts, J.F.; Matthew, J.A.D. Auger parameter studies of aluminium-transition metal alloys. *Surf. Interface Anal.* **2002**, *34*, 360–364. [[CrossRef](#)]
30. Diplas, S.; Shao, G.; Morton, S.A.; Tsakiroopoulos, P.; Watts, J.F. Calculations of charge transfer in Nb–17Al and V–50Al alloys, using the Auger parameter. *Intermetallics* **1999**, *7*, 937–946. [[CrossRef](#)]
31. Diplas, S.; Shao, G.; Tsakiroopoulos, P.; Watts, J.F.; Matthew, J.A. D Calculations of charge transfer in Mg- and Al-transition metal alloys using the Auger parameter. *Surf. Interface Anal.* **2000**, *29*, 65–72. [[CrossRef](#)]
32. Arvanitis, A.; Diplas, S.; Tsakiroopoulos, P.; Watts, J.; Whiting, M.; Morton, S.; Matthew, J. An experimental study of bonding and crystal structure modifications in MoSi<sub>2</sub> and MoSi<sub>2</sub>+xAl (x = 10 to 40 at% Al) via Auger parameter shifts and charge transfer calculations. *Acta Mater.* **2001**, *49*, 1063–1078. [[CrossRef](#)]
33. Diplas, S.; Watts, J.F.; Tsakiroopoulos, P.; Shao, G.; Beamson, G.; Matthew, J.A. D X-ray photoelectron spectroscopy studies of Ti–Al and Ti–Al–V alloys using Cr Kβ radiation. *Surf. Interface Anal.* **2001**, *31*, 734–744. [[CrossRef](#)]
34. Abel, M.-L.; Tsakiroopoulos, P.; Watts, J.F.; Matthew, J.A.D. Free-electron metal alloys: A study by high-energy XPS. *Surf. Interface Anal.* **2002**, *33*, 775–780. [[CrossRef](#)]
35. Diplas, S.; Tsakiroopoulos, P.; Shao, G.; Watts, J.F.; Matthew, J.A.D. A study of alloying behaviour in the Ti–Al–V system. *Acta Mater.* **2002**, *50*, 1951–1960. [[CrossRef](#)]
36. Pankhurst, D.A.; Yuan, Z.; Nguyen-Manh, D.; Abel, M.-L.; Shao, G.; Watts, J.F.; Pettifor, D.G.; Tsakiroopoulos, P. Electronic structure and bonding in, and alloys investigated by X-ray photoelectron spectroscopy and density-functional theory. *Phys. Rev. B* **2005**, *71*, 075114. [[CrossRef](#)]
37. Mitchell, T.; Diplas, S.; Tsakiroopoulos, P.; Watts, J.F.; Matthew, J.A.D. Study of alloying behaviour in metastable Mg–Ti solid solutions using Auger parameter measurements and charge-transfer calculations. *Philos. Mag. A* **2002**, *82*, 841–855. [[CrossRef](#)]
38. Geng, J.; Shao, G.; Tsakiroopoulos, P. Study of three-phase equilibrium in the Nb-rich corner of Nb–Si–Cr system. *Intermetallics* **2006**, *14*, 832–837. [[CrossRef](#)]
39. Utton, C.A.; Papadimitriou, I.; Kinoshita, H.; Tsakiroopoulos, P. Experimental and thermodynamic assessment of the Ge–Nb–Si ternary phase diagram. *J. Alloys Compd.* **2017**, *717*, 303–316. [[CrossRef](#)]
40. Papadimitriou, I.; Utton, C.; Tsakiroopoulos, P. Phase Equilibria in the Nb-Rich Region of Al–Nb–Sn at 900 and 1200 °C. *Materials* **2019**, *12*, 2759. [[CrossRef](#)]
41. Xu, Z.; Utton, C.; Tsakiroopoulos, P. A study of the effect of 2 at.% Sn on the microstructure and isothermal oxidation at 800 and 1200 °C of Nb–24Ti–18Si based alloys with Al and/or Cr additions. *Materials* **2018**, *11*, 1826. [[CrossRef](#)] [[PubMed](#)]



42. Xu, Z.; Utton, C.; Tsakiroopoulos, P. A study of the effect of 5 at.% Sn on the microstructure and isothermal oxidation at 800 and 1200 °C of Nb-24Ti-18Si based alloys with Al and/or Cr additions. *Materials* **2020**, *13*, 245. [[CrossRef](#)]
43. Xu, Z.; Utton, C.; Tsakiroopoulos, P. The Effect of Ge Addition on the Oxidation of Nb-24Ti-18Si Silicide Based Alloys. *Materials* **2019**, *12*, 3120.
44. Hernandez-Negrete, O.; Tsakiroopoulos, P. On the microstructure and isothermal oxidation at 800 and 1200 °C of the Nb-24Ti-18Si5Al-5Cr-5Ge-5Sn (at.%) silicide based alloy. *Materials* **2020**, *13*, 722. [[CrossRef](#)] [[PubMed](#)]
45. Zhao, J.; Utton, C.; Tsakiroopoulos, P. On the Microstructure and Properties of Nb-12Ti-18Si-6Ta-5Al-5Cr-2.5W-1Hf (at.%) Silicide-Based Alloys with Ge and Sn Additions. *Materials* **2020**, *13*, 3719. [[CrossRef](#)]
46. Zhao, J.; Utton, C.; Tsakiroopoulos, P. On the Microstructure and Properties of Nb-18Si-6Mo-5Al-5Cr-2.5W-1Hf Nb-Silicide Based Alloys with Ge, Sn and Ti Additions (at.%). *Materials* **2020**, *13*, 4548. [[CrossRef](#)]
47. Vellios, N.; Keating, P.; Tsakiroopoulos, P. On the Microstructure and Properties of the Nb-23Ti-5Si-5Al-5Hf-5V-2Cr-2Sn (at.%) Silicide-Based Alloy—RM(Nb)IC. *Metals* **2021**, *11*, 1868. [[CrossRef](#)]
48. Thandorn, T.; Tsakiroopoulos, P. On the Microstructure and Properties of Nb-Ti-Cr-Al-B-Si-X (X = Hf, Sn, Ta) Refractory Complex Concentrated Alloys. *Materials* **2021**, *14*, 7615. [[CrossRef](#)] [[PubMed](#)]
49. Kovacic, Z.; Strand, R.; Volker, T. *The Circular Economy in Europe: Critical Perspectives on Policies and Imaginaries*; Routledge: Oxfordshire, UK, 2020.
50. Chen, Y.; Shang, J.-X.; Zhang, Y. Effects of alloying element Ti on  $\alpha$ Nb<sub>5</sub>Si<sub>3</sub> and Nb<sub>3</sub>Al from first principles. *J. Phys. Condens. Matter* **2007**, *19*, 016215. [[CrossRef](#)]
51. Sangiovanni, D.G.; Chirita, V.; Hultman, L. Electronic mechanism for toughness enhancement in Ti<sub>x</sub>M<sub>1-x</sub>N (M=Mo and W). *Phys. Rev. B* **2010**, *81*, 104107. [[CrossRef](#)]
52. Long, Q.; Wang, J.; Du, Y.; Holec, D.; Nie, X.; Jin, Z. Predicting an alloying strategy for improving fracture toughness of C15 NbCr<sub>2</sub> Laves phase: A first-principles study. *Comput. Mater. Sci.* **2016**, *123*, 59–64. [[CrossRef](#)]
53. Yannaras, C. *Person and Eros*; Holy Cross Orthodox Press: Brookline, MA, USA, 2007; ISBN 1-885652-88-7/978-1-885652-88-1.
54. Tsakiroopoulos, P. Alloying and Properties of C<sub>14</sub>-NbCr<sub>2</sub> and A<sub>15</sub>-Nb<sub>3</sub>X (X = Al, Ge, Si, Sn) in Nb-Silicide-Based Alloys. *Materials* **2018**, *11*, 395. [[CrossRef](#)]
55. Tsakiroopoulos, P. On the Nb silicide based alloys: Part I—The bcc Nb solid solution. *J. Alloy. Compd.* **2017**, *708*, 961–971. [[CrossRef](#)]
56. Tsakiroopoulos, P. On the Alloying and Properties of Tetragonal Nb<sub>5</sub>Si<sub>3</sub> in Nb-Silicide Based Alloys. *Materials* **2018**, *11*, 69. [[CrossRef](#)]
57. Tsakiroopoulos, P. Alloying and Hardness of Eutectics with Nbss and Nb<sub>5</sub>Si<sub>3</sub> in Nb-silicide Based Alloys. *Materials* **2018**, *11*, 592. [[CrossRef](#)] [[PubMed](#)]
58. Tsakiroopoulos, P. On the Nb<sub>5</sub>Si<sub>3</sub> Silicide in Metallic Ultra-High Temperature Materials. *Metals* **2023**, *13*, 1023. [[CrossRef](#)]
59. Tsakiroopoulos, P. On Nb silicide based alloys: Part II. *J. Alloys Compd.* **2018**, *748*, 569–576. [[CrossRef](#)]
60. Thandorn, T.; Tsakiroopoulos, P. The effect of Boron on the microstructure and properties of refractory metal intermetallic composites (RM(Nb)ICs) based on Nb-24Ti-xSi (x = 16, 17 or 18 at.%) with additions of Al, Cr or Mo. *Materials* **2021**, *14*, 6101. [[CrossRef](#)]
61. Zacharis, E.; Utton, C.; Tsakiroopoulos, P. A Study of the Effects of Hf and Sn on the Microstructure, Hardness and Oxidation of Nb-18Si Silicide-Based Alloys-RM(Nb)ICs with Ti Addition and Comparison with Refractory Complex Concentrated Alloys (RCCAs). *Materials* **2022**, *15*, 4596. [[CrossRef](#)] [[PubMed](#)]
62. Zacharis, E.; Utton, C.; Tsakiroopoulos, P. A Study of the Effects of Hf and Sn on the Microstructure, Hardness and Oxidation of Nb-18Si Silicide Based Alloys without Ti Addition. *Materials* **2018**, *11*, 2447. [[CrossRef](#)] [[PubMed](#)]
63. Nelson, J.; Ghadyani, M.; Utton, C.; Tsakiroopoulos, P. A Study of the Effects of Al, Cr, Hf, and Ti Additions on the Microstructure and Oxidation of Nb-24Ti-18Si Silicide Based Alloys. *Materials* **2018**, *11*, 1579. [[CrossRef](#)] [[PubMed](#)]
64. Hernández-Negrete, O.; Tsakiroopoulos, P. On the Microstructure and Isothermal Oxidation at 800, 1200 and 1300 °C of the Al-25.5Nb-6Cr-0.5Hf (at.%) Alloy. *Materials* **2019**, *12*, 2531. [[CrossRef](#)]
65. Zhao, J.; Utton, C.; Tsakiroopoulos, P. On the Microstructure and Properties of Nb-12Ti-18Si-6Ta-2.5W-1Hf (at.%) Silicide-Based Alloys with Ge and Sn Additions. *Materials* **2020**, *13*, 1778. [[CrossRef](#)]
66. Ghadyani, M.; Utton, C.; Tsakiroopoulos, P. Microstructures and Isothermal Oxidation of the Alumina Scale Forming Nb<sub>1.7</sub>Si<sub>2.4</sub>Ti<sub>2.4</sub>Al<sub>3</sub>Hf<sub>0.5</sub> and Nb<sub>1.3</sub>Si<sub>2.4</sub>Ti<sub>2.4</sub>Al<sub>3.5</sub>Hf<sub>0.4</sub> Alloys. *Materials* **2019**, *12*, 222. [[CrossRef](#)]
67. Ghadyani, M.; Utton, C.; Tsakiroopoulos, P. Microstructures and Isothermal Oxidation of the Alumina Scale Forming Nb<sub>1.45</sub>Si<sub>2.7</sub>Ti<sub>2.25</sub>Al<sub>3.25</sub>Hf<sub>0.35</sub> and Nb<sub>1.35</sub>Si<sub>2.3</sub>Ti<sub>2.3</sub>Al<sub>3.7</sub>Hf<sub>0.35</sub> Alloys. *Materials* **2019**, *12*, 759. [[CrossRef](#)]
68. Hernández-Negrete, O.; Tsakiroopoulos, P. On the Microstructure and Isothermal Oxidation of Silica and Alumina Scale Forming Si-23Fe-15Cr-15Ti-1Nb and Si-25Nb-5Al-5Cr-5Ti (at.%) Silicide Alloys. *Materials* **2019**, *12*, 1091. [[CrossRef](#)]
69. Hernández-Negrete, O.; Tsakiroopoulos, P. On the Microstructure and Isothermal Oxidation of the Si-22Fe-12Cr-12Al-10Ti-5Nb (at.%) Alloy. *Materials* **2019**, *12*, 1806. [[CrossRef](#)]
70. Tsakiroopoulos, P. On the macrosegregation of silicon in niobium silicide based alloys. *Intermetallics* **2014**, *55*, 95–101. [[CrossRef](#)]
71. Guo, S.; Liu, C.T. Phase stability in high entropy alloys: Formation of solid-solution phase or amorphous phase. *Prog. Nat. Sci. Mater. Int.* **2011**, *21*, 433–446. [[CrossRef](#)]
72. Bewlay, B.P.; Sitzman, S.D.; Brewer, L.N.; Jackson, M.R. Analyses of eutectoid phase transformations in Nb-silicide in-situ composites. *Microsc. Microanal.* **2004**, *10*, 470–480. [[CrossRef](#)]

73. Li, Z.; Tsakiroopoulos, P. On the microstructure and hardness of the Nb-24Ti-18Si-5Al-5Cr-5Ge and Nb-24Ti-18Si-5Al-5Cr-5Ge-5Hf (at.%) silicide based alloys. *Materials* **2019**, *12*, 2655. [[CrossRef](#)]
74. McCaughey, C.; Tsakiroopoulos, P. Type of Primary Nb<sub>5</sub>Si<sub>3</sub> and Precipitation of Nbss in  $\alpha$ Nb<sub>5</sub>Si<sub>3</sub> in a Nb-8.3Ti-21.1Si-5.4Mo-4W-0.7Hf (at.%) Near Eutectic Nb-Silicide-Based Alloy. *Materials* **2018**, *11*, 967. [[CrossRef](#)]
75. Zhang, H.; Zhao, Y.; Huang, S.; Zhu, S.; Wang, F.; Li, D. Manufacturing and Analysis of High-Performance Refractory High-Entropy Alloy via Selective Laser Melting (SLM). *Materials* **2019**, *12*, 720. [[CrossRef](#)]
76. Moravcikova-Gouvea, L.; Moravcik, I.; Pouchly, V.; Kovacova, Z.; Kitzmantel, M.; Neubauer, E.; Dlouhy, I. Tailoring a Refractory High Entropy Alloy by Powder Metallurgy Process Optimization. *Materials* **2021**, *14*, 5796. [[CrossRef](#)]
77. Srikanth, M.; Annamalai, A.R.; Muthuchamy, A.; Jen, C.-P. A Review of the Latest Developments in the Field of Refractory High-Entropy Alloys. *Crystals* **2021**, *11*, 612. [[CrossRef](#)]
78. Senkov, O.N.; Miracle, D.B.; Chaput, K.J.; Couzinié, J.-P. Development and exploration of refractory high entropy alloys—A review. *J. Mater. Res.* **2018**, *33*, 3092–3128. [[CrossRef](#)]
79. Yao, H.W.; Qiao, J.W.; Hawk, J.A.; Zhou, H.F.; Chen, M.W.; Gao, M.C. Mechanical properties of refractory high-entropy alloys: Experiments and modeling. *J. Alloys Compd.* **2017**, *696*, 1139–1150. [[CrossRef](#)]
80. Shang, Y.; Brechtel, J.; Pistidda, C.; Liaw, P.K. *Mechanical Behavior of High-Entropy Alloys: A Review*; Springer: Cham, Switzerland, 2021; pp. 435–522. [[CrossRef](#)]
81. Ye, Y.F.; Liu, C.T.; Yang, Y. A geometric model for intrinsic residual strain and phase stability in high entropy alloys. *Acta Mater.* **2015**, *94*, 152–161. [[CrossRef](#)]
82. Pradeep, K.; Tasan, C.; Yao, M.; Deng, Y.; Springer, H.; Raabe, D. Non-equiatomic high entropy alloys: Approach towards rapid alloy screening and property-oriented design. *Mater. Sci. Eng. A* **2015**, *648*, 183–192. [[CrossRef](#)]
83. Liliensten, L.; Couzinié, J.-P.; Perrière, L.; Hocini, A.; Keller, C.; Dirras, G.; Guillot, I. Study of a bcc multi-principal element alloy: Tensile and simple shear properties and underlying deformation mechanisms. *Acta Mater.* **2017**, *142*, 131–141. [[CrossRef](#)]
84. Zhang, Y.; Yang, X.; Liaw, P.K. Alloy Design and Properties Optimization of High-Entropy Alloys. *JOM* **2012**, *64*, 830–838. [[CrossRef](#)]
85. Oh, H.S.; Kim, S.J.; Odbadrakh, K.; Ryu, W.H.; Yoon, K.N.; Mu, S.; Körmann, F.; Ikeda, Y.; Tasan, C.C.; Raabe, D.; et al. Engineering atomic-level complexity in high-entropy and complex concentrated alloys. *Nat. Commun.* **2019**, *10*, 1–8. [[CrossRef](#)]
86. Chan, K.S. Modelling creep behaviour of niobium silicide in-situ composites. *Mater. Sci. Eng. A* **2002**, *337*, 59–66. [[CrossRef](#)]
87. Suzuki, T. On the Studies of Solid Solution Hardening. *Jpn. J. Appl. Phys.* **1981**, *20*, 449. [[CrossRef](#)]
88. Sha, J.; Hirai, H.; Tabaru, T.; Kitahara, A.; Ueno, H.; Hanada, S. Mechanical properties of as-cast and directionally solidified Nb-Mo-W-Ti-Si in situ composites at high temperatures. *Metal. Mater. Trans. A* **2003**, *34*, 85–94. [[CrossRef](#)]
89. Schneibel, J.; Rawn, C.; Payzant, E.; Fu, C. Controlling the thermal expansion anisotropy of Mo<sub>5</sub>Si<sub>3</sub> and Ti<sub>5</sub>Si<sub>3</sub> silicides. *Intermetallics* **2004**, *12*, 845–850. [[CrossRef](#)]
90. Sekido, N.; Kimura, Y.; Miura, S.; Wei, F.-G.; Mishima, Y. Fracture toughness and high temperature strength of unidirectionally solidified Nb–Si binary and Nb–Ti–Si ternary alloys. *J. Alloys Compd.* **2006**, *425*, 223–229. [[CrossRef](#)]
91. Sha, J.; Yang, C.; Liu, J. Toughening and strengthening behaviour of an Nb-8Si-20Ti-6Hf alloy with addition of Cr. *Scr. Mater.* **2010**, *62*, 859–862. [[CrossRef](#)]
92. Guo, H.; Guo, X. Microstructure evolution and room temperature fracture toughness of an integrally directionally solidified Nb–Ti–Si based ultrahigh temperature alloy. *Scr. Mater.* **2011**, *64*, 637–640. [[CrossRef](#)]
93. Singh, A.K.; Liermann, H.-P. Strength and elasticity of niobium under high pressure. *J. Appl. Phys.* **2011**, *109*, 113539. [[CrossRef](#)]
94. Qi, L.; Chrzan, D.C. Tuning Ideal Tensile Strengths and Intrinsic Ductility of bcc Refractory Alloys. *Phys. Rev. Lett.* **2014**, *112*, 115503. [[CrossRef](#)] [[PubMed](#)]
95. Wang, Y.X.; Geng, H.Y.; Wu, Q.; Chen, X.R.; Sun, Y. First-principles investigation of elastic anomalies in niobium at high pressure and temperature. *J. Appl. Phys.* **2017**, *122*, 235903. [[CrossRef](#)]
96. Christman, T.; Needleman, A.; Suresh, S. An experimental and numerical study of deformation in metal-ceramic composites. *Acta Met.* **1989**, *37*, 3029–3050. [[CrossRef](#)]
97. Grabke, H.J.; Meier, G.H. Accelerated oxidation; internal oxidation, intergranular oxidation and pitting on intermetallic compounds. *Oxid. Met.* **1995**, *44*, 147–176. [[CrossRef](#)]
98. Meier, G.H. Research on oxidation and embrittlement of Intermetallic Compounds in the U.S. *Mater. Corros.* **1996**, *47*, 595–618. [[CrossRef](#)]
99. Shang, C.; Van Heerden, D.; Gavens, A.; Weihs, T. An X-ray study of residual stresses and bending stresses in free-standing Nb/Nb<sub>5</sub>Si<sub>3</sub> microlaminates. *Acta Mater.* **2000**, *48*, 3533–3543. [[CrossRef](#)]
100. Kim, J.-H.; Tabaru, T.; Hirai, H. Evaluation Technique of the Hardness and Elastic Modulus of Materials with Fine Microstructures. *Mater. Trans.* **2003**, *44*, 673–676. [[CrossRef](#)]
101. Bowman, C.; Ritzert, F.; Smialek, J.; Jaster, M.; Barker, S. Compatibility of Niobium alloys and superalloys in a flowing He-Xe power conversion system. In Proceedings of the 2nd International Energy Conversion Engineering Conference, Providence, RI, USA, 16–19 August 2004. [[CrossRef](#)]
102. Mitra, R. Mechanical behaviour and oxidation resistance of structural silicides. *Int. Mater. Rev.* **2006**, *51*, 13–64. [[CrossRef](#)]
103. Zhang, Y.; Zhou, Y.J.; Lin, J.P.; Chen, G.L.; Liaw, P.K. Solid-solution phase formation rules for multi-component alloys. *Adv. En-Gineering Mater.* **2008**, *10*, 534–538. [[CrossRef](#)]

104. Liang, H.; Chang, Y.A. Thermodynamic modelling of the Nb-Si-Ti ternary system. *Intermetallics* **1999**, *7*, 561–570. [[CrossRef](#)]
105. Shao, G. Thermodynamic assessment of the Nb-Si-Al system. *Intermetallics* **2004**, *12*, 655–664. [[CrossRef](#)]
106. Yang, Y.; Bewlay, B.P.; Chang, Y.A. Liquid-Solid Phase Equilibria in Metal-Rich Nb-Ti-Hf-Si Alloys. *J. Phase Equilibria Diffus.* **2007**, *28*, 107–114. [[CrossRef](#)]
107. Geng, T.; Li, C.; Bao, J.; Zhao, X.; Du, Z.; Guo, C. Thermodynamic assessment of the Nb-Si-Ti system. *Intermetallics* **2009**, *17*, 343–357. [[CrossRef](#)]
108. Bulanova, M.; Fartushna, I. Niobium-silicon-titanium. In *Landolt-Börnstein New Series IV/11E3*; Springer: Heidelberg, Germany, 2010.
109. Li, Y.; Li, C.-R.; Du, Z.-M.; Guo, C.-P.; Zhao, X.-Q. As cast microstructures and solidification paths of the Nb-Si-Ti ternary alloys in Nb<sub>5</sub>Si<sub>3</sub>-Ti<sub>5</sub>Si<sub>3</sub> region. *Rare Met.* **2013**, *32*, 502–511. [[CrossRef](#)]
110. Bewlay, B.P.; Yang, Y.; Casey, R.L.; Jackson, M.R.; Chang, Y.A. Experimental study of the liquid-solid phase equilibria at the metal rich region of the Nb-Cr-Si system. *Intermetallics* **2009**, *17*, 120–127. [[CrossRef](#)]
111. Yang, Y.; Chang, Y.A. Thermodynamic modelling of Nb–Cr–Si system. *Intermetallics* **2005**, *13*, 69–78. [[CrossRef](#)]
112. Meschel, S.; Kleppa, O. Standard enthalpies of formation of some 4d transition metal silicides by high temperature direct synthesis calorimetry. *J. Alloys Compd.* **1998**, *274*, 193–200. [[CrossRef](#)]
113. European Commission. *EUROPE 2020: A Strategy for Smart, Sustainable and Inclusive Growth, COM(2010)2020*; European Commission: Brussels, Belgium, 2010.
114. Owen, R.; Macnaghten, P.; Stilgoe, J. Responsible research and innovation: From science in society to science for society, with society. *Sci. Public Policy* **2012**, *39*, 751–760. [[CrossRef](#)]
115. Owen, R.; Stilgoe, J.; Macnaghten, P.; Gorman, M.; Fisher, E.; Guston, D. A framework for responsible innovation. In *Responsible Innovation: Managing the Responsible Innovation of Science and Innovation in Society*; Owen, R., Bessant, J., Heintz, M., Eds.; John Wiley: London, UK, 2013; pp. 27–50.
116. Schomberg, V.R. A vision of responsible innovation. In *Responsible Innovation: Managing the Responsible Innovation of Science and Innovation in Society*; Owen, R., Bessant, J., Heintz, M., Eds.; John Wiley: London, UK, 2013; pp. 51–74.
117. Zelenitsas, K.; Tsakiroopoulos, P. Study of the role of Cr and Al additions in the microstructure of Nb-Ti-Si in situ composites. *Intermetallics* **2005**, *13*, 1079–1095. [[CrossRef](#)]
118. Zelenitsas, K.; Tsakiroopoulos, P. Study of the role of Ta and Cr additions in the microstructure of Nb-Ti-Si-Al in situ composites. *Intermetallics* **2006**, *14*, 639–659. [[CrossRef](#)]
119. Geng, J.; Tsakiroopoulos, P.; Shao, G. The effects of Ti and Mo additions on the microstructure of Nb-silicide based in situ composites. *Intermetallics* **2006**, *14*, 227–235. [[CrossRef](#)]
120. Li, Z.; Tsakiroopoulos, P. The microstructure of Nb-18Si-5Ge-5Al and Nb-24Ti-18Si-5Ge-5Al in situ composites. *J. Alloys Compd.* **2013**, *550*, 553–560. [[CrossRef](#)]
121. Geng, J.; Tsakiroopoulos, P. A study of the microstructures and oxidation of Nb-Si-Cr-Al-Mo In Situ composites alloyed with Ti, Hf and Sn. *Intermetallics* **2007**, *15*, 382–395. [[CrossRef](#)]
122. Vellios, N.; Tsakiroopoulos, P. The role of Fe and Ti additions in the microstructure of Nb-18Si-5Sn silicide based alloys. *Intermetallics* **2007**, *15*, 1529–1537. [[CrossRef](#)]
123. Vellios, N.; Tsakiroopoulos, P. Study of the role of Fe and Sn additions in the microstructure of Nb-24Ti-18Si-5Cr silicide based alloys. *Intermetallics* **2010**, *18*, 1729–1736. [[CrossRef](#)]
124. Fromm, E.; Heinkel, O. The carbon monoxide equilibrium pressure above Ta-C-O solid solution. *Z. Metallk.* **1967**, *58*, 805–810.
125. Fromm, E.; Jehn, H. Thermodynamics and phase relations in refractory metal solid solutions containing carbon, nitrogen, and oxygen. *Met. Trans.* **1972**, *3*, 1685–1692. [[CrossRef](#)]
126. Nguyen-Manh, D. Ab-Initio Modelling of Point Defect-Impurity Interaction in Tungsten and other BCC Transition Metals. *Adv. Mater. Res.* **2008**, *59*, 253–256. [[CrossRef](#)]
127. Ford, D.C.; Zapol, P.; Cooley, L.D. First-principles study of carbon and vacancy structures in niobium. *J. Phys. Chem. C* **2015**, *119*, 14728–14736. [[CrossRef](#)]
128. Blanter, M.S.; Dmitriev, V.V.; Mogutnov, B.M.; Ruban, A.V. Interaction of carbon, nitrogen and oxygen with vacancies and solutes in tungsten. *RSC Adv.* **2015**, *5*, 23261–23270. [[CrossRef](#)]
129. Blanter, M.S.; Dmitriev, V.V.; Mogutnov, B.M.; Ruban, A.V. Interaction of interstitial atoms and configurational contribution to their thermodynamic activity in V, Nb, and Ta. *Phys. Met. Metallogr.* **2017**, *118*, 105–112. [[CrossRef](#)]
130. Ghosh, S.; Ghosh, C. Effect of oxygen interstitials on structural stability in refractory metals (V, Mo, W) from DFT calculations. *Eur. Phys. J. B* **2021**, *94*, 1–9. [[CrossRef](#)]
131. Martin, H.; Abavare, E.K.K.; Amoako-Yirenkyi, P. Thermodynamic stable site for interstitial solute (N or O) in bcc refractory metals (Mo and Nb) using density functional theory. *MRS Adv.* **2022**, *7*, 474–481. [[CrossRef](#)]
132. Xing, H.; Hu, P.; Han, J.; Li, S.; Ge, S.; Hua, X.; Hu, B.; Yang, F.; Wang, K.; Feng, P. Effects of oxygen on micro-structure and evolution mechanism of body-centred-cubic molybdenum. *Int. J. Refract. Met. Hard Mater.* **2022**, *103*, 105747. [[CrossRef](#)]
133. Miura, S.; Ikeda, K.-I.; Takizawa, S.; Watanabe, S. Formation of an onion-like two-phase structure and its effect on mechanical properties of refractory-metal based alloys. In Proceedings of the International Conference Beyond Nickel Based Superalloys IV, Potsdam, Germany, 26–30 June 2023.
134. Bonsteel, R.M.; Rowcliffe, D.J.; Tietz, T.E. Mechanical Properties and Structure of Internally Oxidized Nb-12Zr Alloy. *Trans. Jap. Inst. Met.* **1968**, *9*, 597.

135. Rowcliffe, D.J.; Bonsteel, R.M.; Tietz, T.E. Strengthening of Niobium-Zirconium Alloys by Internal Oxidation. *Met. Soc. Conf.* **1968**, *47*, 741–750.
136. Liu, C.; Inouye, H.; Carpenter, R. *Mechanical Properties and Structure of Oxygen-Doped Tantalum-Base Alloy*; Oak Ridge National Laboratory: Oak Ridge, TN, USA, 1972. [[CrossRef](#)]
137. Fisher, E.S.; Westlake, D.G.; Ockers, S.T. Effect of hydrogen and oxygen on the elastic moduli of vanadium, niobium and tantalum single crystals. *Phys. Status Solidi A* **1975**, *28*, 591–602. [[CrossRef](#)]
138. Wadsworth, J.; Nieh, T.G.; Stephens, J.J. Recent advances in aerospace refractory metal alloys. *Int. Mater. Rev.* **1988**, *33*, 131–150. [[CrossRef](#)]
139. Miura, E.; Yoshimi, K.; Hanada, S. Solid-Solution Strengthening by Oxygen in Nb-Ta and Nb-Mo Single Crystals. *Phys. Status Solidi A* **2001**, *185*, 357–372. [[CrossRef](#)]
140. Sankar, M.; Baligheid, R.; Gokhale, A. Effect of oxygen on microstructure and mechanical properties of niobium. *Mater. Sci. Eng. A* **2013**, *569*, 132–136. [[CrossRef](#)]
141. Zhou, W.; Sahara, R.; Tsuchiya, K. First-principles study of the phase stability and elastic properties of Ti-X alloys (X= Mo, Nb, Al, Sn, Zr, Fe, Co, and O). *J. Alloys Compd.* **2017**, *727*, 579–595. [[CrossRef](#)]
142. Chong, Y.; Poschmann, M.; Zhang, R.; Zhao, S.; Hooshmand, M.S.; Rothchild, E.; Olmsted, D.L.; Morris, J.W.; Chrzan, D.C.; Asta, M.; et al. Mechanistic basis of oxygen sensitivity in titanium. *Sci. Adv.* **2020**, *6*, eabc4060. [[CrossRef](#)] [[PubMed](#)]
143. Liu, C.; Yu, L.; Liu, Y.; Ma, Z.; Li, H.; Li, C.; Liu, C. Interactions between interstitial oxygen and substitutional niobium atoms in Ti-Nb-O BCC alloys: First-principles calculations. *AIP Adv.* **2020**, *10*, 025309. [[CrossRef](#)]
144. Jones, D.W.; McQuillan, A.D. Magnetic susceptibility and hydrogen affinity of bcc alloys of Nb-Mo, Nb-Re and Mo-Re. *J. Phys. Chem. Solids* **1962**, *23*, 1441–1447. [[CrossRef](#)]
145. McLintock, C.H.; Stringer, J. The pressure dependence of the linear oxidation of Niobium in the temperature range 450 °C–1050 °C. *J. Less Common Met.* **1963**, *5*, 278–294. [[CrossRef](#)]
146. Ravi, K.; Gibala, R. The strength of niobium-oxygen solid solutions. *Acta Met.* **1970**, *18*, 623–634. [[CrossRef](#)]
147. Ulitchny, M.; Gibala, R. The effects of interstitial solute additions on the mechanical properties of niobium and tantalum single crystals. *J. Less Common Met.* **1973**, *33*, 105–116. [[CrossRef](#)]
148. Sethi, V.; Gibala, R. Surface oxide softening of Nb and Ta single crystals. *Scr. Met.* **1975**, *9*, 527–531. [[CrossRef](#)]
149. Kassem, M.A.; Koch, C.C. Effect of Interstitials on the Phase Stability of Selected Intermetallics. *MRS Proc.* **1990**, *213*, 801–806. [[CrossRef](#)]
150. Sethi, V.; Gibala, R. Surface oxide softening of niobium single crystals. *Acta Met.* **1977**, *25*, 321–332. [[CrossRef](#)]
151. Duquette, D.J. Environmental resistance of intermetallic compounds. In *Critical Issues in the Development of High Temperature Structural Materials*; Stoloff, N.S., Duquette, D.J., Giamei, A.F., Eds.; International Atomic Energy Agency (IAEA): Vienna, Austria, 1993; pp. 431–443.
152. Rigney, J.D.; Singh, P.M.; Lewandowski, J.J. Effects of environmental exposure on ductile-phase toughness in Niobium-silicide-Niobium composites. *Mat. Res. Soc. Symp. Proc.* **1994**, *322*, 503–509. [[CrossRef](#)]
153. de Souza, A.C.; Grandini, C.R.; Florêncio, O. Effect of heavy interstitials on anelastic properties of Nb-1.0 wt% Zr alloys. *J. Mater. Sci.* **2008**, *43*, 1593–1598. [[CrossRef](#)]
154. Chandran, M.; Subramanian, P.R.; Gigliotti, M.F. Energetics of interstitial oxygen in  $\beta$ -TiX (X=transition metal) alloys using first principles methods. *J. Alloys Compd.* **2013**, *571*, 107–113. [[CrossRef](#)]
155. Inouye, H. Interactions of Refractory Metals with Active Gases in Vacua and Inert Gas Environments. In *Refractory Metal Alloys Metallurgy Technology*; Machlin, L., Begley, R.T., Weisert, E.D., Eds.; Springer: Boston, MA, USA, 1968; pp. 165–195.
156. Ketchum, M.D.; Barrett, C.A. *Contamination of Refractory Metals by Oxygen, Water Vapour and Carbon Monoxide*; NASACR: Daytona Beach, FL, USA, 1970.
157. Hörz, G. Mechanisms and kinetics of absorption and desorption reactions in systems of refractory metals with nitrogen, oxygen or carbon. *Met. Trans.* **1972**, *3*, 3069–3076. [[CrossRef](#)]
158. de Almeida, L.H.; Pires, K.C.C.; Grandini, C.R.; Florêncio, O. Measurement of oxygen atom diffusion in Nb and Ta by anelastic spectroscopy. *Mater. Res.* **2005**, *8*, 239–243. [[CrossRef](#)]
159. Alkamees, A.; Liu, Y.-L.; Zhou, H.-B.; Jin, S.; Zhang, Y.; Lu, G.-H. First-principles investigation on dissolution and diffusion of oxygen in tungsten. *J. Nucl. Mater.* **2009**, *393*, 508–512. [[CrossRef](#)]
160. He, K.-N.; Song, C.; Hou, J.; Xu, Y.-C.; You, Y.-W.; Kong, X.-S.; Liu, C. The influence of transition metal solutes on the dissolution and diffusion of oxygen in tungsten. *J. Nucl. Mater.* **2020**, *537*, 152250. [[CrossRef](#)]
161. Mitchell, J.B. Mechanisms of growth and loss of coherency of HfN particles in Mo. *Acta Met.* **1971**, *19*, 1063–1077. [[CrossRef](#)]
162. Ghosh, G.; Olson, G.B. Integrated design of Nb-based superalloys: Ab initio calculations, computational thermodynamics and kinetics and experimental results. *Acta Mater.* **2007**, *55*, 3281–3303. [[CrossRef](#)]
163. Sabol, S.; Randall, B.; Edington, J.; Larkin, C.; Close, B. *Barrier Coatings for Refractory Metals and Superalloys*; Bettis Atomic Power Laboratory: West Mifflin, PA, USA, 2006. [[CrossRef](#)]
164. Bomchil, G.; Goeltz, G.; Torres, J. Influence of oxygen on the formation of refractory metal silicides. *Thin Solid Films* **1986**, *140*, 59–70. [[CrossRef](#)]
165. Chen, J.; Zhang, X.; Yang, L.; Wang, F. The vacancy defects and oxygen atoms occupation effects on mechanical and electronic properties of Mo<sub>5</sub>Si<sub>3</sub> silicides. *Commun. Theor. Phys.* **2021**, *73*, 045702. [[CrossRef](#)]

166. Zhu, N.; Guo, Y.; Zhang, X.; Wang, F. The effects of vacancies defects and oxygen atoms occupation on physical properties of chromium silicide from a first-principles calculations. *Solid State Commun.* **2021**, *340*, 114535. [[CrossRef](#)]
167. Uttley, J. Study of the Hardness of the Nb Solid Solution and Nb<sub>5</sub>Si<sub>3</sub> Silicide in Nb Silicide Based Alloys Exposed to High Temperatures. Bachelor's Thesis, Final Year Project, University of Sheffield, Sheffield, UK, 2010.
168. Chapman, O. *Study of the Hardness of the Nbss and Nb<sub>5</sub>Si<sub>3</sub> Phases in a Nb Silicide Based Alloy*; Final Year Project; University of Sheffield: Sheffield, UK, 2010.
169. Schlesinger, M.E.; Okamoto, H.; Gokhale, A.B.; Abbaschian, R. The Nb-Si (Niobium-Silicon) System. *J. Phase Equilibria* **1993**, *14*, 502–509. [[CrossRef](#)]
170. Tankov, N. Processing of Niobium Silicide Based Alloys. MPhil Thesis, University of Sheffield, Sheffield, UK, 2023.
171. Encyclopaedia Britannica. Available online: <https://www.britannica.com/> (accessed on 29 January 2023).
172. Tsakiroopoulos, P.; Zelenitsas, K.; Vellios, N. Study of the effect of Al, Cr and Sn additions on the microstructure and properties of Nb silicide based alloys. *MRS Proc.* **2011**, *1295*, 367–372. [[CrossRef](#)]
173. Grammenos, I.; Tsakiroopoulos, P. Study of the role of Hf, Mo and W additions in the microstructure of Nb-20Si silicide based alloys. *Intermetallics* **2011**, *19*, 1524–1530. [[CrossRef](#)]
174. Grammenos, I.; Tsakiroopoulos, P. Study of the role of Mo and Ta additions in the microstructure of Nb-18Si-5Hf silicide based alloy. *Intermetallics* **2010**, *18*, 1524–1530. [[CrossRef](#)]

**Disclaimer/Publisher's Note:** The statements, opinions and data contained in all publications are solely those of the individual author(s) and contributor(s) and not of MDPI and/or the editor(s). MDPI and/or the editor(s) disclaim responsibility for any injury to people or property resulting from any ideas, methods, instructions or products referred to in the content.